DIELECTRIC BREAKDOWN IN SOLIDS

Paul P. Budenstein

Army Missile Research, Development and Engineering Laboratory
Redstone Arsenal, Alabama

20 December 1974

TECHNICAL REPORT RG-75-25

DIELECTRIC BREAKDOWN IN SOLIDS

Dr. Paul P. Budenstein
Physics Department
Auburn University
Auburn, Alabama

20 December 1974

Approved for public release; distribution unlimited.

U.S. ARMY MISSILE COMMAND
Redstone Arsenal, Alabama

PREPARED FOR

Guidance and Control Directorate
US Army Missile Research, Development and Engineering Laboratory
US Army Missile Command
Redstone Arsenal, Alabama 35809

DISPOSITION INSTRUCTIONS

DESTROY THIS REPORT WHEN IT IS NO LONGER NEEDED. DO NOT RETURN IT TO THE ORIGINATOR.

DISCLAIMER

THE FINDINGS IN THIS REPORT ARE NOT TO BE CONSTRUED AS AN OFFICIAL DEPARTMENT OF THE ARMY POSITION UNLESS SO DESIGNATED BY OTHER AUTHORIZED DOCUMENTS.

TRADE NAMES

USE OF TRADE NAMES OR MANUFACTURERS IN THIS REPORT DOES NOT CONSTITUTE AN OFFICIAL INDORSEMENT OR APPROVAL OF THE USE OF SUCH COMMERCIAL HARDWARE OR SOFTWARE.

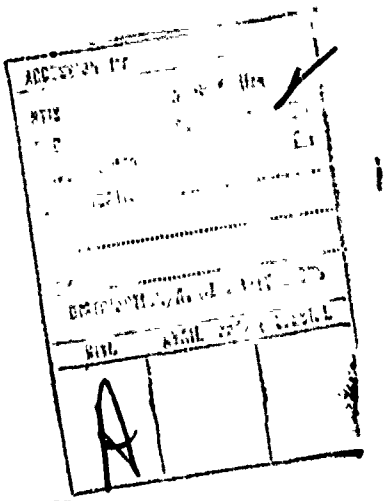

UNCLASSIFIED

SECURITY CLASSIFICATION OF THIS PAGE (When Data Entered)

REPORT DOCUMENTATION PAGE		READ INSTRUCTIONS BEFORE COMPLETING FORM
1. REPORT NUMBER RG-75-25	2. GOVT ACCESSION NO.	3. RECIPIENT'S CATALOG NUMBER AD-A012 177
4. TITLE (and Subtitle) DIELECTRIC BREAKDOWN IN SOLIDS		5. TYPE OF REPORT & PERIOD COVERED Technical Report
		6. PERFORMING ORG. REPORT NUMBER RG-75-25
7. AUTHOR(s) Dr. Paul P. Budenstein, Auburn University		8. CONTRACT OR GRANT NUMBER(s)
9. PERFORMING ORGANIZATION NAME AND ADDRESS US Army Missile Research, Development and Engineering Laboratory US Army Missile Command Redstone Arsenal, Alabama 35809		10. PROGRAM ELEMENT, PROJECT, TASK AREA & WORK UNIT NUMBERS
11. CONTROLLING OFFICE NAME AND ADDRESS		12. REPORT DATE 20 December 1974
		13. NUMBER OF PAGES 54
14. MONITORING AGENCY NAME & ADDRESS(if different from Controlling Office)		15. SECURITY CLASS. (of this report) UNCLASSIFIED
		15a. DECLASSIFICATION/DOWNGRADING SCHEDULE

16. DISTRIBUTION STATEMENT (of this Report)

Approved for public release; distribution unlimited.

17. DISTRIBUTION STATEMENT (of the abstract entered in Block 20, if different from Report)

18. SUPPLEMENTARY NOTES

PRICES SUBJECT TO CHANGE

19. KEY WORDS (Continue on reverse side if necessary and identify by block number)

Dielectric breakdown phenomena
Solids

20. ABSTRACT (Continue on reverse side if necessary and identify by block number)

Experimental and theoretical descriptions of dielectric breakdown phenomena in solids are reviewed. No existing theory seems to adequately explain the range of observed effects. A "new" model of dielectric breakdown is proposed that combines existing mechanisms in a distinctive fashion. The model considers the breakdown process to contain five stages: creation of a critical charge density, bond disruption, chemical chain reaction, growth of a gaseous cavity and crack formation, completion of the gaseous channel bridging the electrodes

DD FORM 1 JAN 73 1473 EDITION OF 1 NOV 65 IS OBSOLETE

UNCLASSIFIED

SECURITY CLASSIFICATION OF THIS PAGE (When Data Entered)

Block 20 Abstract continued

and conduction through this channel. Breakdown conduction is taken to occur only after the solid has been bridged by the gaseous channel. A phenomenological theory is presented for the growth dynamics of the channel. The implications of the entire model are discussed. The model is believed to provide meaningful perspectives concerning the light emission accompanying breakdown, on the geometric configuration of breakdown patterns, on the roles of inhomogeneities, voids and electrode projections, and other significant aspects of breakdown.

CONTENTS

ACKNOWLEDGEMENTS

The author wishes to acknowledge the encouragement of his colleagues at the Redstone Arsenal, D. Mathews, D. Holder, H. Greene, and V. Nieberlein. A rough draft of the manuscript was read by Dr. J. L. Smith and his constructive criticism is appreciated. A portion of the work described in this manuscript has been supported by the Army Research Office; their aid is gratefully acknowledged. Much of the motivation for the breakdown study comes from J. Lloyd, A. Baruah, and J. Knaur of Auburn University. Finally, the author is indebted to Ms. Trish Ray for preparing the final manuscript.

1. Introduction

Dielectric breakdown in solids is an important limiting phenomenon in microcircuits, cables, capacitors, transformers, electrical rotating machinery, particle accelerators and other systems. However, in spite of extensive experimentation and many efforts to explain the breakdown mechanism, none of the theories proposed has been successful in accounting for the broad range of phenomena observed. In this study, we propose a "new" theory that combines existing mechanisms in a distinctive fashion. The resulting conceptual structure is believed to place many of the phenomena associated with breakdown in improved perspective. We first review briefly the experimental evidence and concepts of existing theories, then present the proposed model and examine its implications qualitatively. Quantitative predictions will require additional work.

Whitehead [1] and Mason [2], upon reviewing experimental studies of dielectric breakdown, emphasize that the dielectric strength of materials are quite similar for materials that are structurally very different (for example, mica, quartz, polyethylene, and paraffin); in a test sequence involving each of the above four materials, overlapping ranges can be anticipated. A representative dielectric strength for homogeneous solid insulators is about 10^6 V/cm. Modern work on plastics, crystals, glassy materials, thin films, and composites supports the above observation. Thus dielectric breakdown is not simply associated with the strength of chemical bonding, existence of cleavage planes, melting point, or purity. (This does not mean these factors have no effect, but rather that their role is secondary.)

In breakdown of bulk dielectrics, the damage path bridges the electrodes and frequently contains a main channel and many branching side channels in which the solid has vaporized [3]. (This vaporization, we believe, is a fundamental aspect of the conduction mechanism of dielectric breakdown.) Frequently the channels have a beaded appearance and, for point-plane electrode geometry and single crystal specimens, the channels tend to follow definite crystallographic directions. In partial discharges originating at gas-filled voids, a relatively slow erosion is produced at the wall of the void as the gas is ionized and no breakdown conduction current bridges the electrodes [4].

Dielectric breakdown is always accompanied by light emission. Cooper and his coworkers [5,6,7] have shown that the light emission (attributed to a recombination radiation at impurity centers, but not the ordinary electroluminescence effect) is initiated in KBr crystals 0.5 mm thick about 20 nsec prior to voltage collapse. An intense light is observed about 5 nsec prior to voltage collapse; this light has the same configuration as the breakdown channel. (We interpret this to mean that a gaseous channel is formed prior to voltage collapse.) The

spectrum of light emitted during this formation period has not been determined. However, in time-resolved spectroscopy of the light emitted during breakdown of Al-SiO-Al and other thin film capacitor systems, Budenstein et al. [8] obtained arc spectra, descriptive of atoms in the gaseous state, from the dissociated dielectric and electrode materials. These spectra were obtained from the instant that the voltage waveform indicated the onset of breakdown conduction. (The thin film experiments had a time resolution of tens of nanoseconds.)

Considerable work has been done on the breakdown of transparent insulators by laser irradiation. Agranat et al.[9] find, for 0.69 μm radiation focused into samples of polymethylmethacrylate (PMMA), breakdown thresholds of about 8.5×10^8 W/cm^2 for Q-switched pulses (15 to 20 nsec half width) and analyze a wide variety of measurements on the assumption that the laser irradiation produces, by means not understood, gases at a high temperature (about 6500 K) and high pressure. Light emission, localized to the damage regions, always accompanies laser breakdown. The similarity between laser breakdown and electric breakdown was explored, but the common basis could not be defined. Yablonovitch [10] has explored the common basis in alkali halides, noting similar trends between electric and laser breakdown. He favors an avalanche mechanism as the common initiating factor.

Attempts have been made to relate prebreakdown conduction behavior to breakdown thresholds [11,12], but these have not been successful. Materials of higher dielectric constant, however, seem to have systematically lower breakdown strengths than those with low dielectric constants. The statistical nature of breakdown has been investigated [13]. The delay time for breakdown decreases with overvoltage and the voltage for the onset of breakdown increases with the voltage rise rate [14]. Vorob'ev et al. [12] relate statistical variations in breakdown strength of electrode protrusions, while Klein [15] relates such variations to the probability of developing multiple avalanches.

The forbidden band gap in insulators is typically between 3 and 10 eV. However, as shown by their thermoluminescence and electrical properties, insulators have many discrete energy levels within the band gap which are spatially separated. These levels, which are associated with impurities and imperfections in the lattice structure, serve as trapping and donor sites. Conduction through insulators at room temperature and at high fields is generally believed to involve the relatively free movement of electrons in the conduction band plus trapping of electrons at energy levels in the forbidden gap just slightly below the conduction band. For thin film systems, the electrode-dielectric interface becomes important as a source of electrons. Simmons [16,17] and O'Dwyer [18] have reviewed the electrode-dielectric interface and high field conduction mechanisms (prebreakdown) in detail. Conduction is often strongly influenced by space charge. Watson [19], Bradwell et al. [20], Mukhachev and Mukacheva [21], and others have emphasized the influenced of space charge on breakdown thresholds.

The earliest theories of breakdown hypothesized an ionic motion through the insulator. However, when the rapidity of the breakdown transition was appreciated, attention switched to electronic mechanisms. O'Dwyer [22] has reviewed the theories of von Hippel, Frohlich, Franz, and their followers. The basic theme is that, at sufficiently high fields, electrons in the conduction band can accelerate through the "friction barrier" to energies of about $3/2\ E_g$, where E_g is the width of the band gap. At such energies, the electrons can collide with electrons in the valence band and bring them into the conduction band. Thus the number of electrons in the conduction band is increased. It is shown that this number increases very rapidly with field strength, thus suggesting the reason for the sharp threshold of conduction at breakdown. Electron multiplication (avalanche) theories have yielded predictions on the thickness dependence, the temperature dependence, and the magnitude of the breakdown field.

Unfortunately, the avalanche model does not appear to be consistent with experimental results. If dielectric breakdown occurs through avalanches, then the current through the system should rise before there is destruction. The light emission should occur after the current has had a chance to heat the system and disruption should be thermal in nature. The early development of a gaseous conduction channel and the concommitant line emission spectra do not seem to be at all implied in the avalanche approach to dielectric breakdown.

O'Dwyer [22] also summarizes purely thermal theories of breakdown wherein no new conduction mechanism is hypothesized and Joule heating is responsible for disruption. At elevated temperatures, this seems to describe the observed disruption. At room temperature and below, however, it is easy to perform experiments where heating is negligible up to the breakdown transition. In such experiments the destruction is in the nature of the gaseous channel, whereas the purely thermal case is characterized by blistering, charing, and cracking.

Vorob'ev [23] has suggested that breakdown occurs in thin films because the high current at electrode microprotrusions produces melting of the dielectric films, film decomposition, and the components that determine the conductivity of the discharge channels.

Vershinin [24] proposed a plasma model of breakdown in solids wherein atoms of a gas are created from the solid in a strong static electric field through a resonance process. It is difficult to evaluate this approach since its basic assumptions stem from gaseous plasma theory and many approximations are made. An attempt is made to account for the beaded structure of breakdown channels. Vershinin's direct conversion of a solid to a gas is in marked contrast to the avalanche theories and is consistent with the observations of Cooper and Elliott [5].

2. Proposed Model of Dielectric Breakdown in Solids

a. Concepts of the Model

(1) Critical Charge Density. The basic assumption made is that breakdown occurs when the density of excess charge in an insulator in a local region containing many atoms attains a critical value. The source of this excess charge may be field emission from an electrode, charge multiplication by an avalanche process, charge injection at the surface of an ionized void, electron injection from an external accelerator, electrons produced by ionization processes associated with absorption of laser light, or some other means.

(2) Disruption of Chemical Bonds by Excess Charges. The effect of a charge density greater than critical on the solid is assumed to be disruption of chemical bonds. (Bowden and McLaren [25], in attempting to explain how a relatively small electric field (4.5×10^3 V/m) could initiate an explosive reaction in a single crystal of silver azide, hypothesized that a high local electron density led to the decomposition of the crystal. Subsequent work on silver azide has neither confirmed or disproven this hypothesis [26].)

The mechanism of bond disruption by an excess electron density can be visualized by considering the hydrogen molecule and its ions. An electron can be attached to H_2 to form a stable ion, H_2^-. The three-electron, two-nucleus system (H_2^-) will have a different set of electronic energy levels than the two-electron, two-nucleus system (H_2)[27,28]. (The bond length of H_2 is 0.746 Å, while it is estimated to be 1.65 Å in H_2^-. The H_2 molecule is probably best thought of with the two electrons shared by the two nuclei on an equal basis, while the H_2^- molecule is more like an H weakly coupled to an H^-.) The addition of still another electron to the system [$H_2^- + e \rightarrow H_2^{--}$ (unstable)] leads to a nonbonding situation. This nonbonding may occur with a variety of end products as illustrated in the following chemical reactions:

$$H_2^{--} \rightarrow H + H + 2e \qquad H_2^{--} \rightarrow H_2 + 2e$$

$$H_2^{--} \rightarrow H + H^- + e \qquad H_2^{--} \rightarrow H_2^- + e$$

$$H_2^{--} \rightarrow H^- + H^- \qquad H_2^{--} \rightarrow H_2^+ + 3e$$

$$H_2^{--} \rightarrow H^+ + H^+ + 4e$$

$$H_2^{--} \rightarrow H^+ + H^- + 2e$$

$$H_2^{--} \rightarrow H^+ + H + 3e.$$

The reactions that dominate should be the ones most favorable energetically. These cannot be determined readily from calculations because of the number of particles involved. Note that it is possible to end up with an excess of electrons; i.e., more than 1 electron may be produced in the dissociation of H_2^{--}, whereas only one electron was added to H_2^- to form the unstable H_2^{--}.

(3) Chain Reaction. The third ingredient believed essential to the breakdown process is the chain reaction. A well-known example of a chain reaction is the explosive combination of H_2 and Cl_2 gases [29]. In the absence of light or an electric spark, this mixture is stable at STP. However, a flash of ultraviolet light or a spark will cause the formation of HCl with great rapidity, the reaction being strongly exothermic. The reaction scheme may be represented as follows:

$$H_2 + \text{light} \rightarrow H + H$$

$$H + Cl_2 \rightarrow HCl + Cl$$

$$Cl + H_2 \rightarrow HCl + H$$

$$H + Cl \rightarrow HCl + \text{light}.$$

The reaction products in each case have the potential for causing further reactions; the total energy released is many times the initiating energy. The rate of reaction depends upon the concentrations of the reacting components, temperature, and pressure. These, in turn, depend on the processes of diffusion, loss through boundaries, heat dissipation, wall effects, competing reactions, etc.

In the breakdown problem, we assume that an electron density is created in a local region sufficient to disrupt chemical bonds. Atoms are thus freed from their positions in the solid and form a dense gas. The gas density is the same as that of the solid for an appreciable time. For breakdown to occur, we require that a chain reaction can take place inside the solid so that a gaseous cavity is created with the dissociation products. The reaction sequence as it might occur in crystalline sodium chloride will now be described; the general ideas are believed to be applicable for all types of chemical bonding.

Within solid sodium chloride, the sodium and chlorine atoms exist as ions, Na^+ and Cl^-, respectively. These might be converted to gas atoms having different states of ionization, such as Na^o_{gas}, Na^+_{gas}, Cl^-_{gas}, Cl^o_{gas}, and Cl^+_{gas}, through the reactions:

1) $Na^+_{solid} + e \rightarrow Na^o_{solid} + Q_1$

2) $Na^o_{solid} + Q_2 \rightarrow Na^o_{gas}$

3) $Na^o_{gas} + Q_3 \rightarrow Na^+_{gas} + e$

4) $Cl^-_{solid} \rightarrow Cl^-_{gas} + Q_4$

5) $Cl^-_{gas} + Q_5 \rightarrow Cl^o_{gas} + e$

6) $Cl^o_{gas} + Q_6 \rightarrow Cl^+_{gas} + e.$

Reactions 3), 5), and 6) occur in the gaseous state and are activated by collisions among the particles of the gas. The entire reaction scheme must be highly exothermic if the chain reaction is to be vigorous.

The above reaction scheme is depicted in a two-dimensional format in Figure 1. Figure 1a shows a region with a single extra electron. This might stay trapped for an appreciable time, but would not cause lattice disruption. In Figure 1b, the electron density is increased so that the ionic charges on several nearest-neighbor sodium atoms are neutralized as indicated in reaction step 1) (note the five central sodium atoms in the figure). Because of their thermal energies, the neutralized sodium atoms [reaction step 2)] can move with ease from their former equilibrium positions (Figure 1c). The neutral sodium atoms experience only slight binding energy to their former equilibrium positions. [Reaction step 2) should occur more readily at high temperatures, suggesting that the breakdown strength should decrease with increasing temperature.] The movement of the sodium atoms removes the constraints on the adjacent Cl^- atoms. Figure 1d shows the system after the Cl^- atoms have moved, through their mutual repulsion, from their equilibrium positions [reaction step 4)]. In so doing they lose some potential energy and gain kinetic energy; thus, by subsequent collisions, they heat up the gas created by the atoms that have left their equilibrium positions. Figures 1e and 1f show how the electron density in the gas can be built up through further collisions [reaction steps 3), 5), and 6)]. Finally, in Figure 1g, the second stage of the chain reaction is depicted after the excess electron density has caused more sodium atoms to be freed from the solid matrix.

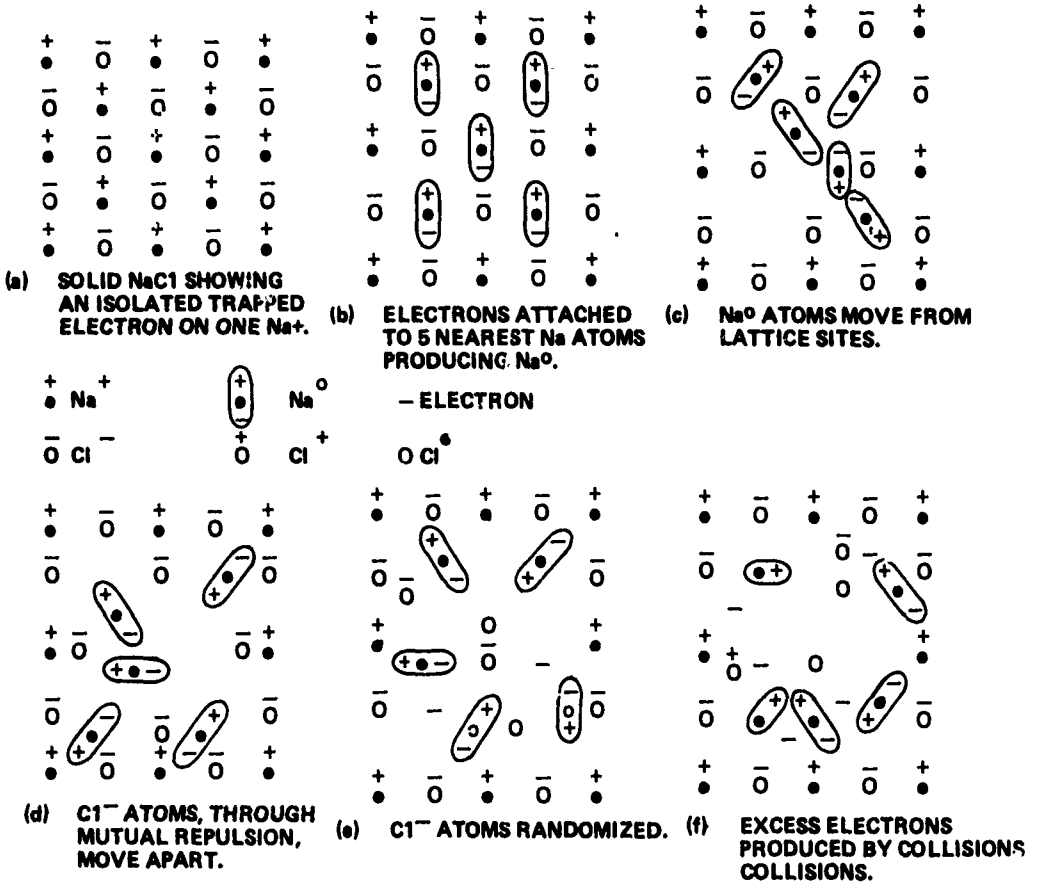

Figure 1. Schematic description of the bond disruption and chain reaction in NaCl.

Note that the reaction sequence has the capability of releasing more electrons than were needed for initiation and hence has the potential for a chain reaction. The nature of the mechanism is believed to be quite general: nonbonding should occur whenever the local density of electrons is made too high, regardless of the detailed nature of the chemical bond.

(4) Establishment of a Gaseous Conducting Channel. The result of the chain reaction is the conversion of the solid in a local region to a partially ionized gas. As the chain reaction proceeds, a gaseous cavity is formed within the solid. The reactions must take place with great rapidity because sufficient energy must be continually added to the gas to compensate for heat transfer to the surrounding medium. As the size of the cavity increases, the medium about the cavity is subjected to very high stresses and cracks will start to form. As they form, new surface area is exposed and the chain reaction spreads to this, thus maintaining the high pressure.

(5) Completion of the Channel. We assume that the breakdown conduction current starts when a gaseous channel bridges the electrodes. The currents prior to this are associated with high field prebreakdown conduction mechanisms; these are assumed incidental to breakdown except as they give rise to a high local space charge density that can initiate the chain reaction. If the gaseous channel cannot completely bridge the electrodes during the time in which the voltage is applied, then the system experiences a "partial breakdown", one in which damage has occurred without completion of the conducting path. If the gaseous channel does bridge the electrodes, conduction through the channel begins since the gas is ionized. As conduction proceeds, further erosion of the walls can occur because of the high electron density and the heating of the plasma by the external circuit. Experimentally, the conductivity of the system in the breakdown region changes by a factor of about 10 [10] in a time of about 10 nsec, measured from the observed beginning of the gaseous channels to the onset of breakdown conduction [5,30].

b. Simplified Theory for the Growth of a Gaseous Channel

The reaction kinetics of real systems depend on the detailed reactions present. As was shown for the hypothesized reactions for breakdown in NaCl, many reactions are possible during the dissociation and recombination processes associated with creation of the gaseous channel. In a dielectric that is chemically complex, many more dissociative and recombinatorial processes would be involved. However, one of the significant features of dielectric breakdown is that the breakdown fields for homogeneous specimens of different materials are remarkably similar. Thus it becomes plausible to think in terms of a model having highly simplified chemical kinetics. Such a model will be outlined in this section. The solutions for this model, which depend on the treatment of the heat flow problem and detailed assumptions on kinetic coefficients have not yet been explored.

We assume that the critical density of charge necessary for initiating the chain reaction is present; the proposed theory is intended to describe the growth of the gaseous cavity. The rate of reaction wherein the solid is converted to gas is assumed to depend upon the electron density n_e in the gas and on the wall area of the cavity. For each molecule removed from the solid, some neutral atoms, positive ions, negative ions, and electrons are added to the gas. Each material will have its own peculiar distribution of these reaction products. Also, there is some total energy released, partially as kinetic energy of the individual particles and partially as electron excitation, when a molecule of the solid is converted to the gaseous phase. In our simplified model, we describe the breakup without identifying the atomic species present. When an average molecule breaks away from the solid, we will say that a certain number of neutrals, positive ions, negative ions, and electrons are added to the gas. Atomic and ionic species will not be further differentiated; i.e., an atom of sodium in the gas will be treated the same as an atom of chlorine in the gas, a positive sodium ion the same as a positive chlorine ion, etc. For purposes of describing the gas, we will assume its mass density is the same as that of the solid and the average volume per atom in the gas is the same as the average volume (volume of a molecule in the solid/No. of atoms in one molecule) of an atom in the solid.

We define wall generation coefficients for describing the dissociation at the cavity walls as follows:

1) α_+ = fraction of wall atoms released as positive ions

2) α_- = fraction of wall atoms released as negative ions

3) α_o = fraction of wall atoms released as neutrals

4) α_e = fraction of the number of wall atoms of electrons released at the wall.

The wall generation coefficients are assumed to be independent of the gas parameters. For simplicity the ions are assumed to be singly ionized.

The gas (neutrals, positive ions, negative ions, and electrons) is a dynamic system. Particles are added continuously and the volume of gas increases as the solid is eroded. At any instant the cavity gas will be assumed to be sufficiently close to equilibrium values that there is meaning to speaking of temperature, pressure, and particle concentrations as system parameters. Since there is heat flow from the cavity gas while the cavity is growing, the temperature and pressure will vary with time. Thus the densities of neutrals, positive ions, negative ions, and electrons (n, n_+, n_-, and n_e, respectively) will vary through the processes of recombination, electron attachment and

detachment, and ionization within the gas. The volume processes and their kinetic coefficients are as follows:

1) Ionization of neutrals, kinetic coefficient β_1

neutral → (+ ion) + electron

2) Recombination, kinetic coefficient γ_1

(+ ion) + electron → neutral

3) Charge transfer from a negative ion to a positive ion, kinetic coefficient γ_2

(- ion) + (+ ion) → 2 neutrals

4) Charge exchange between two neutrals, kinetic coefficient γ_3

neutral + neutral → (+ ion) + (- ion)

5) Electron attachment to a neutral, kinetic coefficient γ_4

electron + neutral → (- ion)

6) Electron detachment from a negative ion, kinetic coefficient β_2

(- ion) → electron + neutral.

The kinetic coefficients are functions of temperature and pressure.

The equations that determine the state of the cavity system are taken to be the following:

1) Charge neutrality condition

$$n_e + n_- = n_+$$

2) Constancy of density of solid and gas

$n_+ + n_- + n = a_v$, where a_v = number of atoms per unit volume of the solid

3) Rate of growth of the cavity:

a) The dielectric is assumed isotropic and the cavity spherical. The electron density is taken to be uniform at all points on the surface of the cavity. The number of particles added to the cavity per unit time is assumed proportional to the electron density in the cavity and the wall area; that is,

$$d(a_v V)/dt = k n_e 4\pi r^2$$

where V is the volume of the cavity, r is the cavity radius, and k is a proportionality constant.

b) The proportionality constant is assumed to be independent of the gas parameters. n_e is one of the dependent variables of the system and its value as a function of time is part of the solution. Thus, using $V=(4/3)\pi r^3$, the above equation can be integrated to obtain r at any time t. The result is

$$r = (k/a_v) \int_0^t n_e(t)\, dt \quad .$$

4) Rate equations:

a) Positive ions

$$dn_+/dt = \alpha_+ k n_e 4\pi r^2 + \beta_1 n + \gamma_3 n^2 - \gamma_1 n_+ n_e - \gamma_2 n_+ n_-$$

b) Negative ions

$$dn_-/dt = \alpha_- k n_e 4\pi r^2 + \gamma_4 n_e n + \gamma_3 n^2 - \beta_2 n_- - \gamma_2 n_+ n_-$$

c) Neutrals

$$dn/dt = \alpha_o k n_e 4\pi r^2 + \gamma_1 n_+ n_e + \gamma_2 n_+ n_- + \beta_2 n_- - \gamma_4 n_e n - \beta_1 n - \gamma_3 n^2$$

d) Electrons

$$dn_e/dt = \alpha_e k n_e 4\pi r^2 + \beta_2 n_- + \beta_1 n - \gamma_1 n_+ n_e - \gamma_4 n n_e$$

5) Heat flow from cavity to surroundings:

a) The temperature of the cavity changes according to the balance between the energy added due to the wall reactions and the energy conducting into the surrounding medium. The heat capacity of the cavity gas becomes strongly temperature-dependent when the temperature is high enough to excite electrons and produce ionization.

$$kn_e 4\pi r^2 \epsilon_a = c(T)\ M\ dT/dt + dQ/dt \quad ,$$

where ϵ_a is the average energy released into the gas per atom converted to gas at the walls, c(T) is the specific heat capacity of the gas, M is the mass of gas in the cavity at time t, T is the temperature of the cavity gas, and dQ/dt is a negative quantity, the heat flow from the gas to the surrounding medium.

b) The heat flow from the gas to the surroundings is determined by solving the heat conduction equation for the spherically symmetric system with the heat flow to the surrounding medium equal to dQ/dt in the above equation. The heat conduction equation for spherical symmetry is

$$\frac{\partial T}{\partial t} = \varkappa \left[\frac{1}{r^2} \frac{\partial}{\partial r} \left(r^2 \frac{\partial T}{\partial r} \right) \right] \quad .$$

c) The temperature at the cavity surface is the same as that inside the cavity. (A detailed solution using the heat conduction equation is probably unattainable, but a simplified "law of cooling," such as Newton's law of cooling, might work adequately.)

The initial conditions are:

$$\text{at } t = 0, \quad r = 0,\ n_+ = 0,\ n_- = 0,\ n = 0,\ n_e = (n_e)_{CRIT} \quad .$$

Here, $(n_e)_{CRIT}$ is the charge density necessary to initiate the chain reaction.

The method of solution is numerical integration. First, reasonable values must be chosen for the coefficients. The temperature dependence of the β's and γ's and c(T) are required. The constraint equations,

$$n_e + n_- = n_+ \quad \text{and} \quad n_+ + n_- + n = a_v \quad ,$$

can be used to eliminate two of the four dependent variables in two of the rate equations. Thus, we might eliminate n_+ and n_- in the rate equations for n_e and n. The n_e and n rate equations would have to be solved simultaneously with the cavity size equation and the heat flow equations. Ultimately, the solution would give the cavity temperature as a function of time, the cavity radius as a function of time, $n_e(t)$ and n(t). With these quantities and using the constraint conditions in the rate equations for n_+ and n_-, each of these equations can be expressed in terms of one dependent variable and functions of time and numerically integrated.

3. Discussion

a. Strength of Chemical Bonds

If the proposed model is to be of general nature, there must be considerable similarity in the strength of chemical bonds and in the ease of bond rupture by electrons. In this section bond strengths, both valence and ionic, are examined briefly.

Table 1 presents data to provide perspective on the strength of chemical bonds of stable systems. These data suggest that about 4 eV is the energy required to remove an atom from a diatomic molecule, from a polyatomic molecule, or from a crystal. The 4 eV assumes the atom is neutral and far from the atoms to which it was formerly bonded. In practice, "far" means several atomic spacings.

b. Electron-Induced Dissociation

Since the proposed mechanism for breakdown is based on electron-induced dissociation, it is appropriate to examine the evidence for such reactions. Fortunately, electron-induced reactions have been extensively studied during the past 30 years [31]. In such studies, monoenergetic electrons are directed into gas molecules in an ionization chamber and the products of the interaction are analyzed with a mass spectrometer. Generally there is a threshold electron energy required before any reaction occurs. Then (Figure 2) there is a narrow energy range where electrons are captured and they cause dissociation of the molecules. Because of the narrowness of the energy range, this is called a resonance reaction. At a considerably higher energy range, the electrons behave more as projectiles and cause dissociation without capture of the electron. The mechanism of dissociation can be understood in terms of the potential energy curves of the ions for different internuclear distances when the molecule is in different electronic states. Field and Franklin [31] illustrate this as shown in Figure 3. Curves a, b, c, and d represent the potential energies of molecules when the electrons are in different states of excitation. States a, b, and c have equilibrium positions, each at a different internuclear separation. According to the Franck-Condon principle, electronic transitions take place so rapidly that the internuclear distance does not change during the transition. Thus, in Figure 3, the transitions occur along the vertical lines (constant internuclear distance). The internuclear distance for a given electronic state is not a constant because the nuclei vibrate about their center of mass. The probability of finding the nuclei with a particular internuclear distance is shown in the figure for several vibrational states. If the transition takes place when the system is in electronic state a and with smallest internuclear separation, a range of vibrational energies are possible for the transition to electronic state b without producing dissociation. If this energy is exceeded, then dissociation will occur. If the transition were to state c, the molecule would probably dissociate because of the

TABLE 1. STRENGTH OF CHEMICAL BONDS (FROM HANDBOOK OF CHEMISTRY AND PHYSICS, '54TH EDITION, 1973-1974, CRC PRESS, CLEVELAND, OHIO)

Diatomic Molecules			Comments
H-H	104 kcal/mol	4.50 eV/mol	Most diatomic molecules have a bonding strength between 40 and 120 kcal/mol (1.73 and 4.80 eV/mol).
H-F	136	5.90	
H-Cl	103	4.47	
H-I	71	3.17	
Li-F	138	6.14	
Li-Cl	112	4.98	
Li-Br	100	4.34	
Li-I	85	3.78	
C-O	257	11.3	
N-N	227	9.86	
O-O	119	5.16	
O-Si	184	7.98	
O-Fe	96	4.17	
Cl-K	101	4.39	
Polyatomic Molecules			
H-OH	119	5.16	Most bond strengths in polyatomic molecules cover the same range of bond strengths as diatomic molecules.
H-N_3	85	3.69	
O-NO	73	3.17	
O-SO	125	5.43	

Lattice Energies of Alkali Halides (kcal/mol)

Elements	Fluoride	Chloride	Bromide	Iodide	
Lithium	240.1	199.2	188.5	174.1	The lattice energy of 183.1 kcal/mol for NaCl is equivalent to 7.94 eV/mol or 3.97 eV/atom.
Sodium	213.4	183.1	174.5	163.9	
Potassium	189.7	165.4	159.3	150.8	
Rubidium	181.6	160.7	153.5	145.3	
Cesium	173.7	152.2	146.3	139.1	

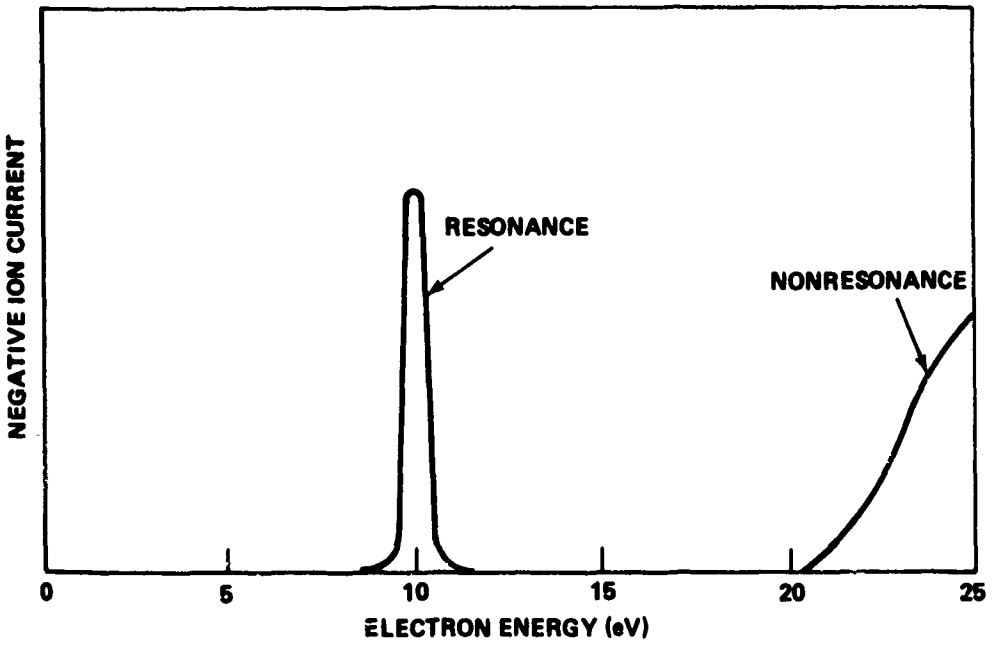

Figure 2. Dissociation due to electron impact of CO molecules. [The resonance reaction is $CO + e \rightarrow C + O^-$. The nonresonance is $CO + e \rightarrow C^+ + O^- + e$ (after Field and Franklin)].

large amount of vibrational energy even though there is a minimum in the potential energy curve of state c. State d contains no minimum in its potential energy curve, so an electronic transition to this state would always produce dissociation. If the transition from state a occurred when the internuclear distance corresponded to the equilibrium position of classical oscillators, stable transitions could exist over an energy range both to states b and c. The same would be true if the transition occurred at the maximum separation of the nuclei in state a.

In both resonant and nonresonant reactions, the final products typically emerge with some kinetic energy. This kinetic energy has been measured for the ions, but not the neutrals. The amount of kinetic energy is a function of the incident electron energy, but there is generally a minimum kinetic energy for a particular molecule-electron interaction. Field and Franklin list reactions and the minimum kinetic energy of the ions in each. The following is a sampling from their data:

$$O_2 + e \rightarrow O^+(0.25\ eV) + O + 2e$$

$$CO + e \rightarrow O^+(0.3\ eV) + C + 2e$$

$$CO + e \rightarrow O^- + C \text{ (no kinetic energy for the resonance case)}$$

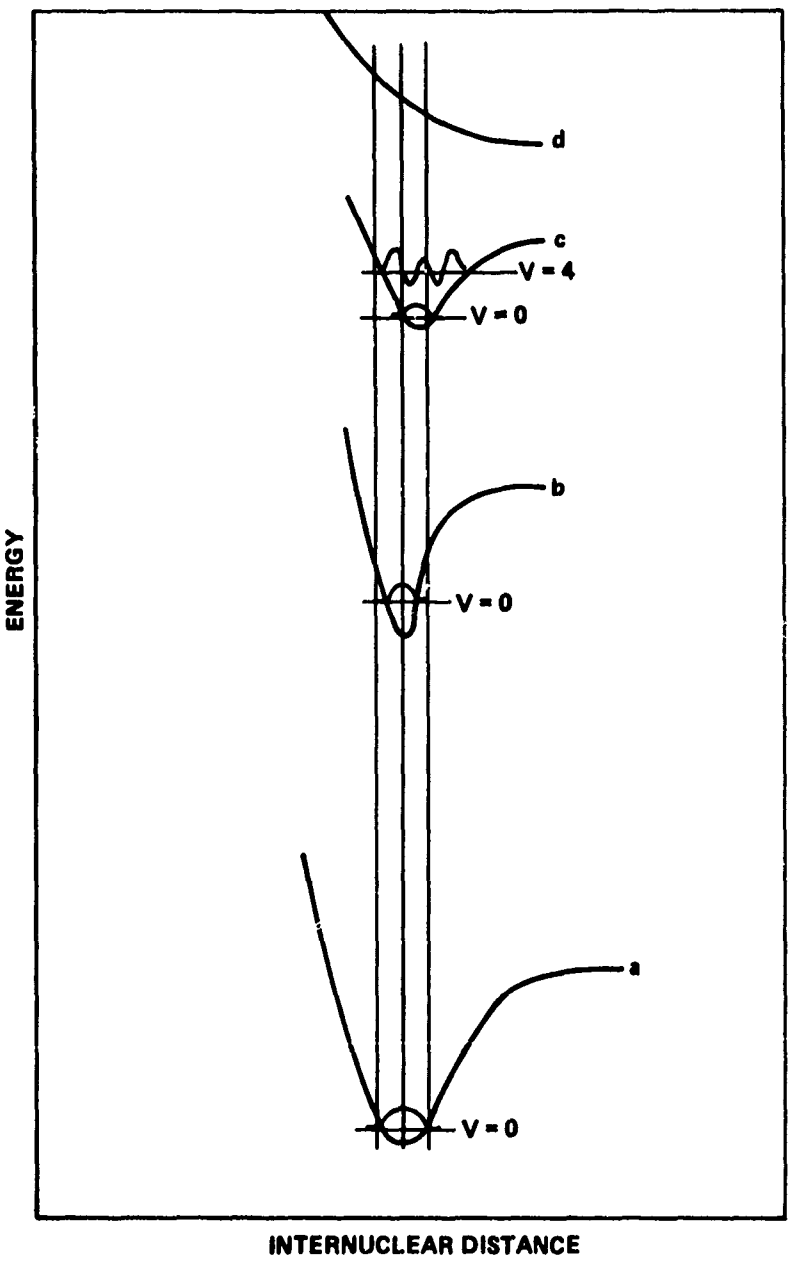

Figure 3. Potential energy curves for a diatomic molecule for different states of electronic excitation (after Field and Franklin).

$$NO + e - O^-(0.9\ eV) + N$$

$$O_2 + e \rightarrow O^-(1.7\ eV) + O$$

$$Br_2 + e \rightarrow Br^-(2.3\ eV) + Br$$

$$C_3H_8 + e \rightarrow CH_3^+(1.99\ eV) + C_2H_5$$ (CH_3^+ from 14 hydrocarbons had a minimum kinetic energy that ranged from 1.6 to 4.6 eV).

The data on minimum kinetic energy of ions from dissociated molecules suggest that 1 eV is a representative value. Average values for resonance reactions are probably twice this amount or more.

It is appropriate to indicate how the electron-molecule reactions just described differ from the electron-induced reactions envisaged in the proposed model. The nonresonance reactions involve energy and momentum transfer from the incident electron to the system particles, but the energy level structure of the system is determined by the original molecule. In the resonance reaction, the incident electron is captured and the energy level structure of the system is modified. Dissociation would occur with the total energy of the system distributed as translational and electronic excitations of the separate particles. The solid reactions due to excess electrons are believed to be similar to the resonance reactions; the added electrons are believed to appreciably modify the local energy level structure. (Work on this point is currently in progress by J. Lloyd.)

The slow deterioration (aging) of insulators under the long-term action of relatively weak electric fields is generally associated with the presence of voids, macroscopic particles, or electrode protrusions. The deterioration process seems to be explainable as an electron-induced dissociation. For slow deterioration, the rate of electron production must be too small to initiate a chain reaction but large enough, on occasions, to cause bond disruption. The macroscopic particle might cause electron injection by field emission if it is a conductor or by ionization of a small gaseous pocket associated with it.

c. Parameters of the Conducting Channel

(1) Average Energy of Atoms. In the last section, evidence was presented from electron-molecule (gas) reactions that the average energy per atom when chemical bonds are broken is several electron volts. In the experimental observations of light emission during breakdown conduction in thin film capacitors, radiation in the ultraviolet is observed (a wavelength of 2000 Å corresponds to 6.2 eV) [8]. Moreover, the observed spectrum is a line spectrum and not a thermal one and it is observed from the very beginning of breakdown conduction. Thus, although there must always be some highly excited neutrals and ions (those freshly created), the gas must have an effective

temperature that is much less than that corresponding to several electron volts of energy per atom. Still, th. gas temperature must be several kilokelvins if the gas is not to condense; the input energy to the gas must be sufficient to offset the energy loss by heat conduction from the gas to the surrounding medium.

An estimate of the heat transfer from the gas to the surrounding medium is needed. Carslaw and Jaeger [32] treat a problem similar to the one in question. They determine the heat flow and temperature-time history of a region outside of a perfectly conducting circular cylinder. (We can think of the gas in a breakdown channel as being the perfectly conducting cylinder in the model.) In the calculation the temperature outside the cylinder is initially constant and chosen to be zero, while the temperature of the cylinder is taken initially as an elevated value of T_o. Analytical expressions are given for the temperature distribution outside the cylinder as a function of time and for the temperature within the cylinder as a function of time. Also graphical data are presented describing the temperature-time history of the conducting cylinder. The time history depends on the heat capacity of the conducting cylinder as well as that (and other thermal properties) of the surrounding medium. If the conducting cylinder contains gas at very high temperature and pressure, its specific heat capacity must include translational motion, electronic excitation and interparticle forces. In the temperature and pressure ranges of interest, the specific heat capacity of the solid is probably between 0.5 and 1 times the specific heat capacity of the gas.

Table 3 shows the times required for the temperature within the cylinder to fall to 0.1 T_o for cylinder radii of 10, 100, and 1000 Å and for specific heat capacities in the range of interest. The times can be construed as representative if the initial temperature were several tens of kilokelvins and the temperature of 0.1 T_o were several kilokelvins. The times are seen to be extremely short for the smaller radii.

Temperature versus time, rate of change of temperature versus time, and required reaction rate versus time are plotted in Figures 4, 5, and 6 for several values of T_o, cylinder radius and specific heat ratio. By "required reaction rate" in Figures 4c, 5c, and 6c we mean the number of particles per unit time that must be converted from solid to gas, assuming each particle contributes 2 eV of energy to the gas and the cylinder has a length equal to its radius. From Figure 4, if T_o = 20,000°K for a cylinder of 100 Å radius and equal specific heats of gas and solid, at a time of 0.01 nsec, the temperature is about 5400°K, the rate of temperature fall is 2.95×10^5°K/nsec, and the required reaction rate is 500×10^7 particles/nsec. If the cylinder radius were

TABLE 3. TIMES FOR THE TEMPERATURE OF A PERFECTLY CONDUCTING CYLINDER, ORIGINALLY AT A TEMPERATURE T_o ABOVE THAT OF THE SURROUNDING MEDIUM, TO FALL TO 0.1 T_o. [TIMES ARE GIVEN IN TERMS OF TWO PARAMETERS, "a" THE CYLINDER RADIUS AND "b" THE RATIO OF THE HEAT CAPACITIES OF THE TWO MEDIA ($b = c_{sur}/c_{cyl}$).]

b	(a = 10 Å) Time (nsec)	(a = 100 Å) Time (nsec)	(a = 1000 Å) Time (nsec)
1	0.0004	0.04	4
0.75	0.0006	0.06	6
0.50	0.0010	0.10	10

changed to 1000 Å, the other parameters being the same as above, then (Figure 5) at a time of 1 nsec the cylinder temperature is about 5400°K, the rate of temperature decrease is 2900°K/nsec, and the required reaction rate for a cylinder of 1000 Å length is 5×10^7 particles/nsec.

The reaction rates of Figures 4, 5, and 6 are so large that one is forced to question whether any known chemical systems react at such rates. Some insight can be gained by considering the rate of burning of a solid rocket propellant, a surface reaction (as is the breakdown reaction) that leads to the conversion of solid to gas. The rate of burning of a propellant is typically a function of the pressure, the rate usually increasing with increasing pressure. A representative propellant burns at a rate of about 2×10^{19} particles/(m^2-nsec) at 2000 psi, where a "particle" is an atom of the propellant. An "explosive" system reacts typically about five times as fast as this. The data of Carslaw and Jaeger indicate a heat transfer rate of 10^{-4} J/m-nsec is representative for a cylinder radius of 1000 Å. The rate at which particles must be supplied from the wall of the cylinder is

$$\text{No. of particles released from wall per unit area per unit time} = \frac{\text{Heat transfer per unit length per unit time}}{\text{Wall area per unit length} \times \text{Energy released per particle}}$$

$$= \frac{10^{-4}\ \text{J/m-nsec}}{2\pi 10^{-7}\ \text{m}^2/\text{m} \times 2(1.60 \times 10^{-19})\ \text{J/part}}$$

$$\approx 5 \times 10^{20}\ \text{particles/m}^2\text{-nsec}.$$

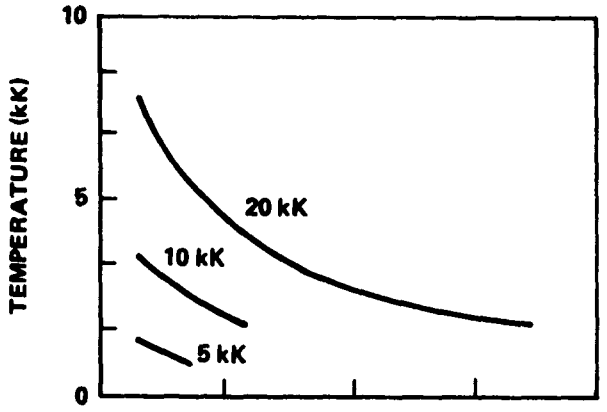

(a) CYLINDER TEMPERATURE VERSUS TIME

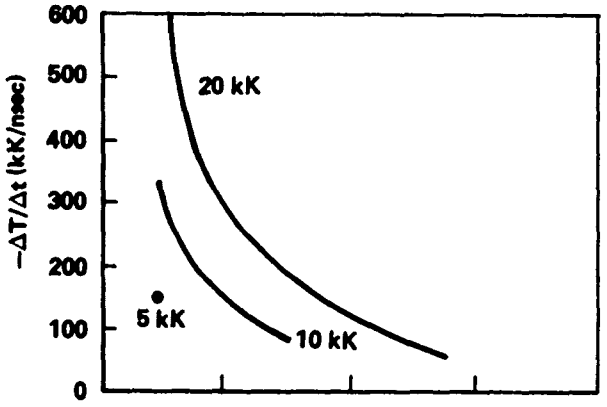

(b) RATE OF DECREASE OF CYLINDER TEMPERATURE VERSUS TIME

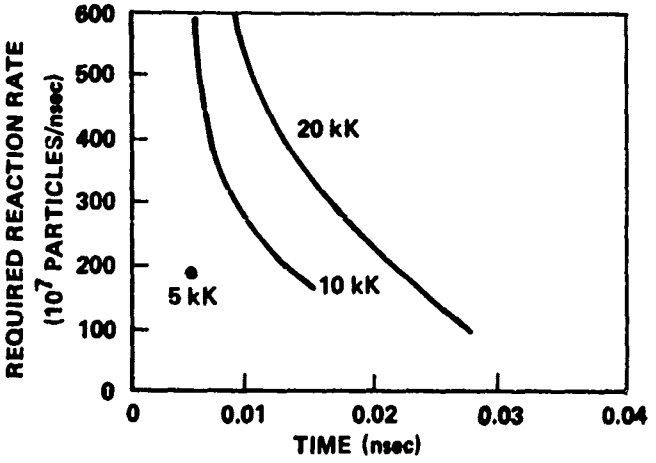

(c) REQUIRED REACTION RATE TO COMPENSATE FOR HEAT TRANSFER ASSUMING A CYLINDER 100 Å LONG AND AN AVERAGE ENERGY PARTICLE OF 2 eV.

Figure 4. Heat transfer from cylinder of 100 Å radius, b = 1. (Parameter on each curve is T_o.)

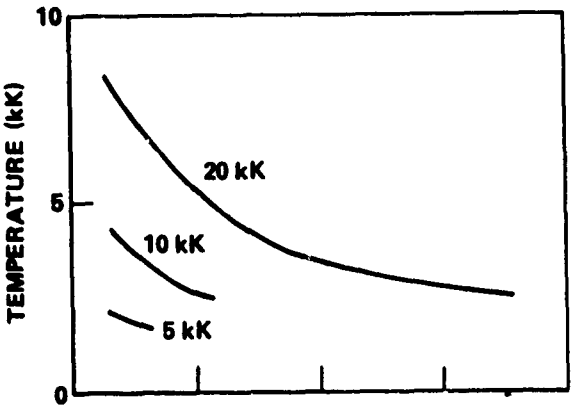

(a) CYLINDER TEMPERATURE VERSUS TIME

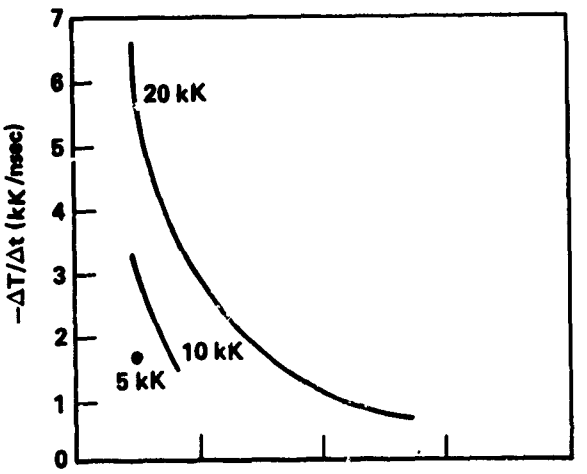

(b) RATE OF DECREASE OF CYLINDER TEMPERATURE VERSUS TIME

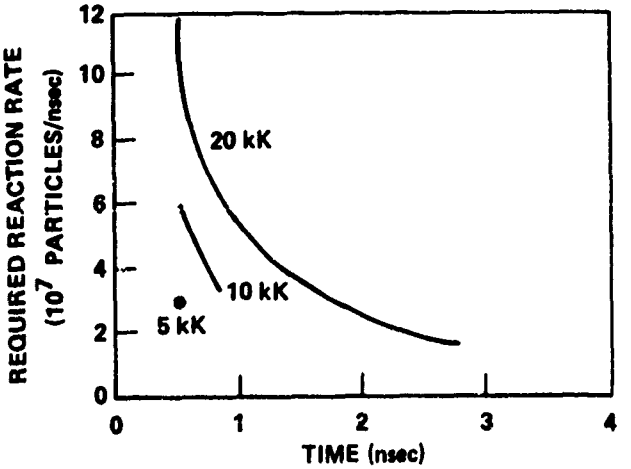

(c) REQUIRED REACTION RATE TO COMPENSATE FOR HEAT TRANSFER ASSUMING A CYLINDER 1000 Å LONG AND AN AVERAGE ENERGY PER PARTICLE OF 2 eV

Figure 5. Heat transfer from cylinder of 1000 Å radius, b = 1. (Parameter on each curve is T_o.)

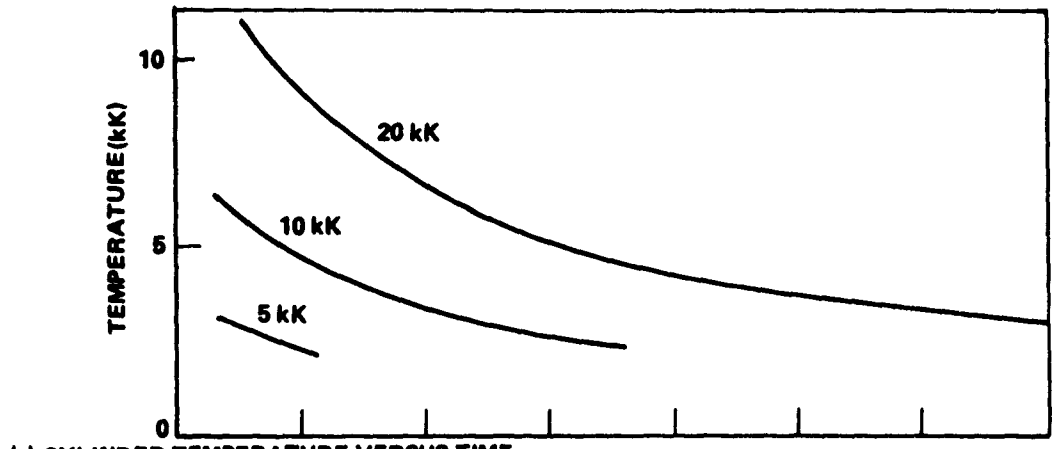

(a) CYLINDER TEMPERATURE VERSUS TIME

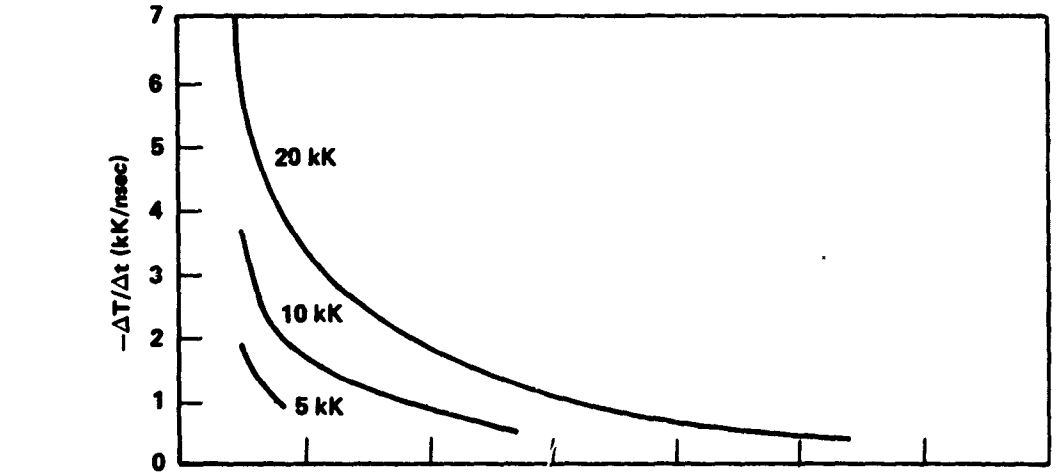

(b) RATE OF DECREASE OF CYLINDER TEMPERATURE VERSUS TIME

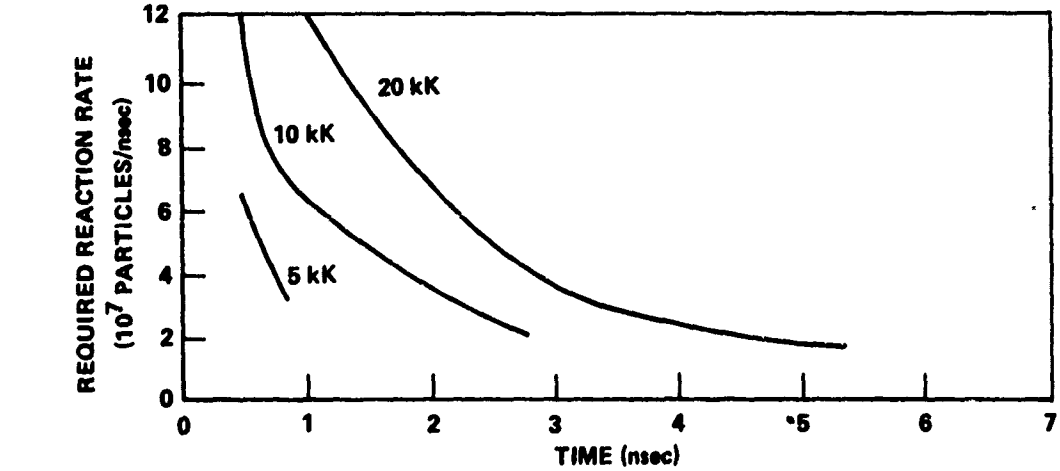

(c) REQUIRED REACTION RATE TO COMPENSATE FOR HEAT TRANSFER ASSUMING A CYLINDER 1000 Å LONG AND AN AVERAGE ENERGY ENERGY PER PARTICLE OF 2 eV.

Figure 6. Heat transfer from cylinder of 1000 Å radius, b = 1/2. (Parameter on each curve is T_o.)

Since the pressure in the gas is estimated to be about 10^6 or 10^7 psi, the above reaction rate is not unreasonable. If the cylinder radius were 100 Å and the time 0.01 nsec, the reaction rate would have to be higher by a factor of 100. For a cylinder of radius 10 Å and a time of 0.0001 nsec, the reaction rate would have to increase by another factor of 100.

The very high reaction rates required to balance the heat loss during the time that a breakdown channel is developing indicate that dielectric breakdown is probably the most rapid chemical reaction in nature. The time scales associated with the different size channels can be inferred to be less than those of Table 3. Thus the time for the cavity to reach a radius of 10 Å is probably less than 10^{-12} seconds, to reach 100 Å probably less than 10^{-10} seconds, and to reach 1000 Å probably less than 10^{-8} seconds.

(2) Temperature. The highly excited atoms and ions that give rise to the observed line spectra are probably those just freshly added to the cavity gas, emission occurring as part of the thermalizing process. Most of the cavity gas must be at a temperature sufficient to maintain the gaseous state, but low enough to produce little blackbody radiation. Measurement of the blackbody spectrum would be very desirable as a direct measurement of the gas temperature. The temperature of the gas will be approximately 6000°K and the average energy per gas particle about 0.5 eV.

(3) Pressure. The gas pressure is believed to be an important dynamic channel parameter because it leads to crack formation and propagation. These will be discussed further in connection with breakdown geometry. If the average energy per atom is 0.5 eV and the gas density is the same as that of the solid, then the pressure is about 3×10^{10} Pascals (4×10^6 psi). Zlatin et al. [33] have measured the velocity of the shock wave produced in plexiglas as the discharge channel grew radially. They applied a 650 kV pulse to embedded electrodes located 4 mm apart and measured after the gaseous channel had formed and during the period of Joule heating and continued channel erosion. During this period, the channel pressure was estimated to be about 30 kbar (4.4×10^5 psi). This value should be less than the pressure in the period of growth of the primary channel.

(4) Electrical Conductivity. The electrical conductivity of the gas in the discharge channel depends primarily on the free electron density. Since the chain reaction must continue throughout the entire channel until the gaseous channel bridges the electrodes, each portion of the channel continues to supply electrons. If the chain reaction were to cease locally, the temperature of the gas in that region would rapidly fall and the gas would solidify, possibly in the disordered structure of a glass. Davisson [3] indicates that

the conductivity of a gaseous channel that bridges the electrodes is sufficiently small that little further damage is done by Joule heating after the channel is completed if thick specimens and low overvoltages are employed. Thus the system is self-ballasted. For thin specimens, it is necessary to insert a protective series resistance to limit the current if the channel is not to be greatly eroded after its formation. (A thin specimen in this context is a few tenths of a millimeter in thickness or less, while a thick specimen is about 1 mm thick.) In thin film studies, conduction during breakdown generally occurs at constant resistance and it is possible to estimate the resistivity of the breakdown channel. Taking the channel diameter to be 40 μm, the dielectric thickness 0.2 μm and the channel breakdown resistance 40 ohms [8], the channel resistivity is about 0.2 ohm-m. This value of resistivity would give the channels of Davisson's thick specimens a resistance in the neighborhood of 10^6 ohms.

The constant resistance of breakdown channels in thin film studies indicates that the conduction mode, once established, does not change appreciably during the period of breakdown conduction. Since gaseous conduction exists in several forms (Townsend discharge, streamers, arcs), this means that the gaseous channel forms prepared to conduct. The state of ionization of the gas suggests that the mode of conduction is the arc. However, unlike the free arc in a typical gaseous discharge, this arc is tightly bounded by the walls of the solid.

d. Perspectives Provided by the Proposed Model

(1) Dependence of Breakdown on the Mode of Excitation.

The damage to dielectrics subjected to electrical stresses, high energy electron beams, and laser beams is sufficiently similar that common mechanisms appear to be involved. Thus it is appropriate that each of these be examined in the light of the proposed breakdown model.

(a) Breakdown Damage Configurations Under Electric Excitation. Davisson [3] has made detailed studies of breakdown geometry in single crystal specimens and has summarized his own work and that of others in a definitive review. He distinguishes the main types of breakdown paths and interprets their modes of formation as follows:

"1) Partial-breakdown paths:

a) Partial-breakdown paths are formed in inhomogeneous electrical fields such as are produced by point electrodes and are characterized by the fact that they can terminate within the dielectric. They are produced by either dc or pulsed voltage, but it is advantageous to use pulsed voltage since secondary destructive effects are avoided. In crystals, a single pulse frequently yields a family of partial breakdown paths which lie along equivalent crystallographic directions. Such a family of equivalent paths is termed a

configuration. A different configuration may be obtained when the conditions of breakdown are changed, but for a given crystal all configurations have a common symmetry and we call this the symmetry of its breakdown pattern.

b) Since partial paths can terminate within the crystal, they can have exceedingly small cross sections. Thus the paths can frequently be followed beyond the limit of resolution of a microscope when oblique (dark field) illumination is used. In general, the positive and negative partial paths have the same physical appearance and cannot be distinguished visually. The partial paths are either bidirectional or unidirectional. The distinction here is whether a path can form, grow, or propagate along a line in either direction or only in one direction. The paths are either straight, segmented, or curved; and their orientation is either precise, sharp, rough, poor, or random. They are beaded hollow channels with circular cross-sections.

c) It is believed that the paths are formed in the following way. Due to certain events, the material within the channel becomes molten and partially vaporized. Upon cooling, the liquid column breaks to form a series of beads lying within a hollow channel. There is usually no observable alteration of the crystal outside the channel. The partial path is understood to have a primary or secondary origin depending upon whether or not its formation is due to oriented electron (or hole) avalanches.

2) Surface breakdown paths: Surface breakdown paths are partial-breakdown paths which lie on the free surface of the crystal. They are observed under the microscope as fine scratches or traces on the surface.

3) Rupture paths: Certain crystals do not yield partial-breakdown paths from a point but always fail catastrophically with the formation of a single, broad, random path of disruption that penetrates the sample. Such paths are termed rupture paths.

4) Homogeneous field paths: Breakdown paths, formed in thin crystal plates, which follow the direction of the applied homogeneous electrical field and are not oriented by the crystal are homogeneous field paths. Paths that are oriented by the crystal, irrespective of the direction of the applied field, are oriented paths.

5) Metallic dendrites: Dendrites are metallic growths resembling trees that originate at point electrode(s) and grow within certain heated crystals when subjected to moderate electric fields."

The discussion that follows will focus on the geometric aspects of point-plane breakdown in crystals exhibiting directional effects. Figure 7a and 7b, from Davisson, show, a schematic of a star pattern in LiCl and a photograph of a star pattern in LiF, respectively. The actual patterns are three-dimensional, the center of the star being at one surface of a slab and the extremities being on the opposite surface. The beaded appearance of the configuration in the photograph is clear. The work of Cooper and Elliott (subsequent to the studies of Davisson) suggests that Davisson's explanation (see his description of partial-breakdown above) for the beaded appearance is incorrect, the beads having formed during the creation of the channel.

Both the beaded appearance and the star configuration can be understood in terms of the proposed model, Griffith's theory of crack propagation, and the anisotropy of the ultimate strength of a crystal. The star patterns are formed when a point-plane electrode geometry is used and the radial aspect reflects the diverging field lines from the pointed electrode. In a typical experiment, the point is very sharp and the local mechanical stress close to the point is high. We imagine that the critical charge density occurs inside the dielectric close to the pointed electrode and, hence, a high-pressure, gaseous cavity starts to form. If the material is anisotropic, the cavity will not be spherical in shape but will tend to elongate in directions of easy erosion. The high pressure gas will exert a compressive stress on the surrounding medium. Ultimately the cavity will reach a critical size so that the stress it exerts on the surrounding medium exceeds the material strength along certain crystallographic directions and a microscopic crack will form in these directions.

According to Griffith's theory of crack propagation, a crack will form when the work required to separate the atoms is equal to the sum of the work done by the external force and the decrease in strain energy resulting from the crack formation. The stress required for crack formation is estimated to be about one-tenth of Young's modulus for the material [34]. The gas pressure estimate given in the previous section is somewhat higher than this. Steverding [34] shows that the incubation time for fracture decreases approximately as the inverse of the stress for high stresses. Further, for high stresses applied for times shorter than a critical time (about 100 nsec), very little energy goes into the deformation of the medium and practically all energy goes into breaking the intermolecular bonds that constitute the fracture. Yokobori [35] comes to similar, though less quantitative, conclusions.

The conditions leading to formation of cracks as the volume of the gaseous region increases are depicted schematically in Figure 8. Although the pressure drops somewhat because of the increase in volume accompanying the formation of a crack, the reaction zone is extended to the new region because of the high density of electrons in the gas. The mechanical stress should be highest at the apex of the crack and molecular bonding weakest. Hence the reaction rate there should be

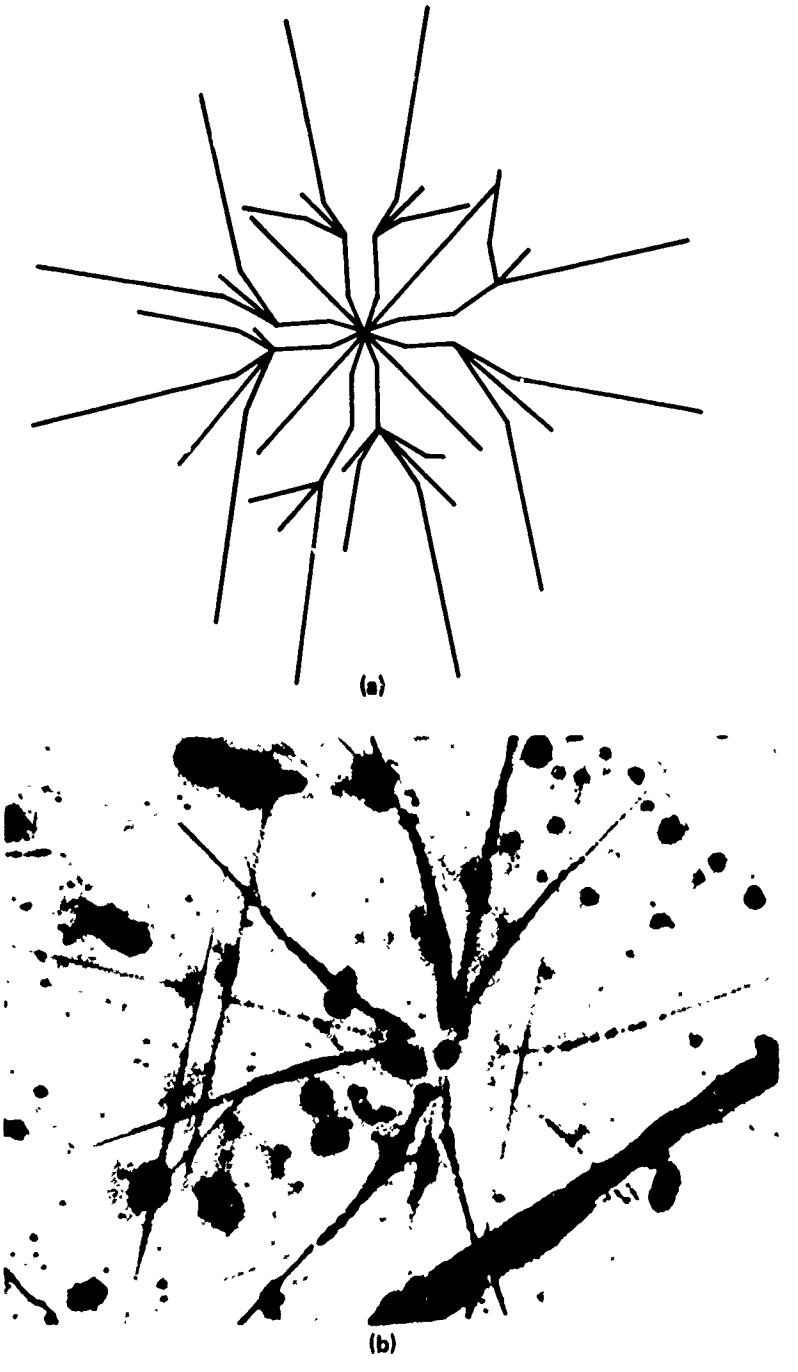

Figure 7. (a) Typical star pattern in lithium chloride and lithium bromide (after Davisson). (b) Overvoltage star pattern in lithium fluoride. The overvoltage paths terminate within the crystal and are replaced by paired paths corresponding to ordinary breakdown which carry the discharge to the bottom of the sample. The diameter of this pattern is about 0.5 mm. The beam diameter is estimated to be several μm and the bead spacing is about 5 μm (after Davisson).

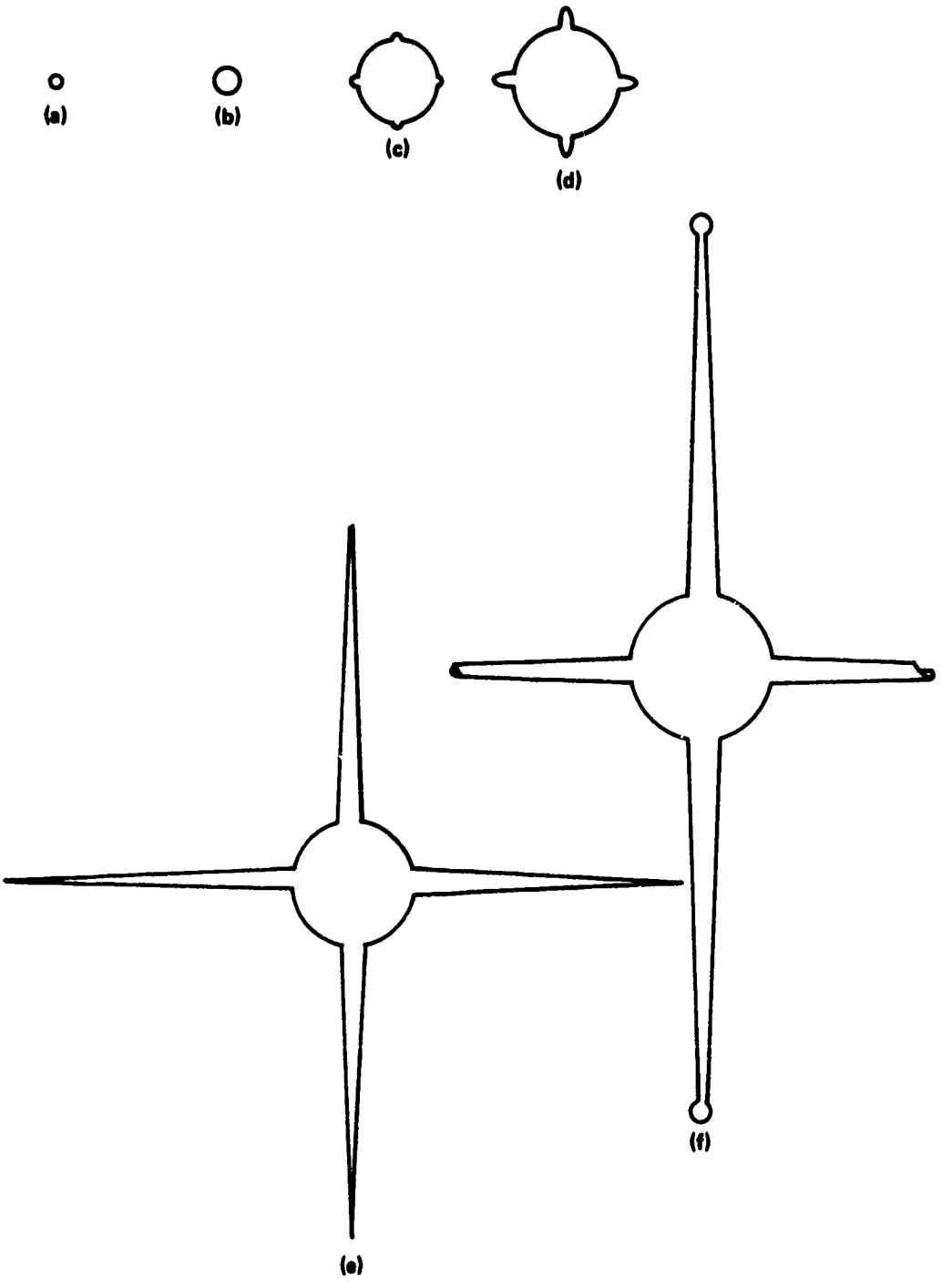

Figure 8. Top view of a dielectric slab (schematic) showing how a gas cavity might grow in an anisotropic medium. [Growth proceeds going from (a) through (f). Crack formation is depicted in (e) and growth of new beads in (f). The cracks occur in equivalent crystallographic directions and are inclined toward the plane electrode.]

highest. Thus the apex will tend to be the center of a new cavity (bead). Since the gas in the channel is a good conductor relative to the surrounding medium, the apex will also be a region of very high field and high electron density. Eventually, the gaseous cavity at the apex enlarges to the point where the stress that it causes in the surrounding medium can no longer be tolerated and another crack or series of cracks will form. The apex cavity will have experienced some bias in its growth because of the anisotropy of the crystal and the local variations in electron density. If the anisotropy of the strength is the dominating factor, the channel should continue to grow in a particular crystallographic direction. If the anisotropy were smaller, the electric field would play a more dominant role and a curved path would more likely occur. As the above process is repeated, the beaded channels form. At some point, the combination of electric field direction and medium anisotropy might make a different set of crystallographic directions more favorable. Then branching of the channel would occur.

In the above description, channel growth is described as a stepwise process. Examination of the photograph of Figure 7b indicates that not all of the channels have a beaded appearance. The nonbeaded channels seem to occur when the total channel volume is relatively large. Further, the nonbeaded channels are of relatively small cross section, so their formation does not appreciably alter the gas pressure. Thus they maintain a nearly constant stress on the surrounding medium, allowing them to continue to propagate without stops.

If the supply voltage were terminated before the discharge channel reached through the material, no conduction current would occur through the channel and the system would be left with a partially formed channel. This is very plausible for the proposed model, but the explanation of such partial discharge channels on the basis of an electron multiplication model does not seem possible.

Cooper and Elliott [36] studied directional effects in annealed and unannealed KCl single crystals using double-recess electrodes, the field being applied in the [110] direction. With strained specimens, the breakdown channel occurred in the [110] direction. For annealed specimens, the breakdown channel was 45 degrees away from the field direction and in the [100] direction. Cooper and Elliott conclude "the existence of electronic instabilities in directions other than the direction of the applied field also appears to rule out breakdown theories of the hot-electron type ... In this type of theory inter-electronic collisions are assumed to be much more numerous than electron-phonon collisions, thus one would not expect the electron cloud to be preferentially directed by the lattice." In the model of breakdown proposed, the direction of the breakdown channel is a compromise determined by the direction of the applied field and the strength anistropy of the medium. Thus the role of strain is to reduce the strength anisotropy.

(b) Breakdown Damage Under Electron Beam Excitation. Dielectric breakdown can occur when electron beams in the MeV range are injected into dielectric slabs. The phenomena are somewhat different depending upon the nature of the electron beams. We distinguish between the low current, continuous beam of the van de Graaff generator [37] and the high current, pulse beam of the flash x-ray generator [38].

If the beam of a van de Graaff generator is used to irradiate a slab of lucite or similar plastic several inches in diameter and about an inch thick, the beam covering one face of the slab, breakdown can occur either during irradiation or later, depending upon the dosage and subsequent treatment. If breakdown occurs during irradiation, there is no convenient way of separating the role of the kinetic energy of the high energy injected electrons in the breakdown process from that of space charge and electric field effects. However, when breakdown occurs later, the kinetic energy of the incident beam can no longer be a factor. Milton [38] has irradiated a slab of lucite so that breakdown occurred during irradiation, as shown in the photograph of Figure 9. The slab was then removed from the irradiation chamber and the other two breakdowns of Figure 9 were produced by gently tapping the surface of the slab with a grounded center punch. In all three cases, the tree-like breakdown pattern was confined to a plane parallel to the irradiated surface and at a depth corresponding to the penetration of the injected electron beam. Most of the damage to the polymer structure produced by the beam itself occurs close to this plane. Thus the plane of breakdown damage is perpendicular to the incident electron beam and virtually perpendicular to the electric field associated with the injected space charge and induced charges on the center punch and ground plane. The damage channels went from the center punch contacts to the layer containing most of the injected charge, then laterally (parallel to the irradiated face) to the edge of the slab.

If electric breakdown were due to an electron avalanche mechanism, the breakdown path should be parallel to the electric field in an isotropic medium. Thus the breakdown damage should be primarily from the charge layer to the surface (the conductivity in the plane of the injected space charge prior to breakdown is very low; charges can remain for many hours or longer). As Figure 9 shows, the appearance of the discharges, whether they occurred during irradiation or subsequently, are qualitatively the same. Thus the kinetic energy of the incident beam did not play a significant role in the breakdown. Further, the spread of the pattern in a direction that is virtually perpendicular to the field seems inexplicable on the basis of an avalanche model. On the other hand, the proposed model provides a good basis for explaining the pattern of damage. Each discharge, according to the model, initiated when the critical charge density was reached in a local region (the pressure wave produced by the center punch, according to this, had to cause such a condition from the existing space charge). Dissociation, chain reaction and growth of a gaseous pocket followed. Growth of the discharge path in the damage layer of the incident beam occurred because of the mechanical weakening of this layer and the presence of a high charge density.

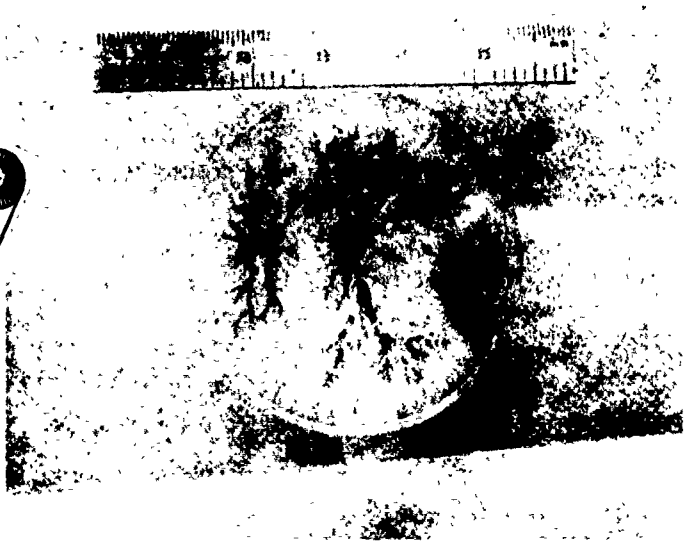

Figure 9. Photograph of electron beam induced breakdown in a lucite slab 0.75-in. thick. The entire face was irradiated with a 1-2 MeV electron beam. The central breakdown occurred during irradiation, while the other two breakdowns were induced later by impacting with a grounded center punch. For the breakdown on the left, the center punch was on the upper face of the slab. For the breakdown on the right, the center punch was on the side of the slab. All breakdown patterns were concentrated in a thin layer about 0.25 in. below the top surface.

The beam of a 2 MeV flash x-ray unit is of short duration (about 50 nsec), high intensity (about 10^{15} electrons per burst), and relatively small cross-section (about 1 cm^2). Thus the number of electrons per unit area in a single burst is about the same as the number of atoms per unit area in a single layer of a solid. (This does not imply that all of the incident electrons are stopped within one atomic layer, but it does suggest a very high density of excess charge is produced inside the slab by a single pulse.) Dielectric breakdown will be induced by such a pulse, the breakdown channel being a random path to the surface of the dielectric (not confined to a plane parallel to the irradiated face). The channel can be directed to a particular region by use of a pointed grounded electrode.

An analysis of the light emission accompanying beam-induced breakdown and a comparison of this with the light emission from breakdown in the same material using electric excitation would be of interest in establishing the common basis of the mechanisms. Similar spectra should be observed if the proposed model is correct.

(c) Damage in Dielectrics Due to Laser Irradiation. Agranat, et al. [9] studied the damage thresholds in polymethylmethacrylate (PMMA), polystyrene (PS), and polycarbonate (PC) plastics with the basic aim of determining the reasons for the threshold intensities and to establish a damage criterion. They employed Q-switched pulses of 15 to 20 nsec duration (half-power) (with energy up to 1 J and wavelengths of 0.69 and 1.06 μm) and picosecond pulses (5×10^{-11} seconds, energy up to 0.1 J, and wavelength of 0.69 μm). Damage occurred at a given wavelength in a particular material when the product of the energy per unit area E and power per unit area J at the damage site was equal to a constant. For 0.69 μm radiation in PMMA for single nanosecond pulses, the threshold occurs at an energy density E_p of 17 J/cm^2 and power density J_p of 8.5×10^8 W/cm^2, yielding a product $J_p E_p$ of 1.4×10^{10} J-W/cm^2. This same product holds for picosecond pulses and repetitive nanosecond subthreshold pulses, the latter requiring multiplication of the energy density-power density product of each pulse by the number of pulses that must be applied to yield damage ($nJ_n E_n$). In the subthreshold tests a sequence of pulses was applied and visible damage, production of cavities 50 to 100 μm in diameter, appeared suddenly with the last pulse of a series. The damage due to the nanosecond pulses was in the form of a relatively small number of fairly large (50 to 100 μm) cavities, with cracks sometimes emanating a short distance from the cavities. In picosecond pulse damage, a large number of very small cavities were produced, each about 1 μm in diameter. These were randomly arranged or in lines (in the latter case, the density is about 10^4/cm).

The study of Agranat et al. leads to conclusions very similar to those of our breakdown model. Hence, we quote their article in length:

> "The large number of damaged areas arising under the action of picosecond pulses shows that there is a large number of microdefects (about 10^{12} per cm^3) that act as nuclei for the formation of damage. This circumstance forces us away from the assumption that the damage originates at foreign inclusions, although these can be of some importance. The thermophysical properties, for example, of PMMA and PS are such that for the transformation of the same quantity of each polymer into gas almost the same amount of energy is required, whereas their threshold values differ by a factor or two.
>
> These polymers differ both by their thermophysical characteristics and structure and by their microstructural characteristics. We shall establish that these differences show up in the magnitude of the damage threshold. To this end we changed the microstructure of the PMMA samples by stretching them to produce a strong orientation. In oriented samples the microstructural elements are strongly elongated along the orientation

direction and the mechanical strength perpendicular to this direction is about 1.5 times less than in unoriented PMMA; this indicates a decrease in the bonding between the structural elements. The experiments showed that in oriented PMMA, the planes of fractures are arranged along the direction of orientation and the threshold value of the laser pulse $\tilde{J}_{pl}$ is less than in unoriented samples J_{pl}; $\tilde{J}_{pl}=0.63\ J_{pl}$; the damage criterion remained the same. This suggests that the threshold values are determined by the magnitude of the coupling between the structural elements.

In (Ref. 5,6) it was solidly established that the damaging cracks arise under the action of a gas that is formed at certain points of the irradiated region. The damage criterion, to begin with, indicates that the character of gas formation is non-thermal. To find out whether the destruction was by electrical breakdown, we did some experiments on damage by a laser with plane and circular polarizations. In these experiments the energy and intensity remained constant, but the field changed by a factor of 1.4. The threshold values of the laser pulses remained unchanged.•••Thus, mechanical destruction of PMMA samples evoked by the action of laser radiation is not caused by an electrical breakdown in the sample induced by the electromagnetic field of the laser radiation.

It is known that under the action of laser radiation the formation of damaging cracks in polymer samples is accompanied by light emission (1,5,6). Our experiments further showed that the emission is localized in microregions and, judging from the cooling time (decrease of emission intensity), the linear dimensions of the microregions are of the order 0.4 μm (above the damage power density threshold). For $J < J_p$ (J = power density, J_p = power density at damage threshold for a single pulse), the intensity of the emission repeats the shape of the incident pulse, and its maximum value is about an order of magnitude smaller than the maximum intensity under the action of laser pulses with $J \geq J_p$. If a series of pulses with $J_n < J_p$ acts on the sample, then at the moment of damage formation (last pulse of the series) the intensity of the emission increases by an order of magnitude. The intensity of the emission evoked by the action of laser pulses with $J \geq J_p$ has a thermal character ($T = 6500$ K) and is independent of the intensity of the laser pulses in the range $J_p \leq J \leq 3J_p$. The emission ($J > J_p$) arises 10 ns after the cracks begin to grow and develops 'independently'—the maximum intensity does not coincide with the laser pulse maximum. We carefully checked the possibility that the laser caused luminescence in the sample. •••We conclude that this light does not come from luminescence of the sample or impurities in it.

Our results can therefore be summarized as follows.

1. There exist threshold values of the laser pulses (for $\tau \approx 2 \times 10^{-8}$ sec) and a damage criterion, which does not depend on the duration of the pulses but does depend on the wavelength of the light field, with a numerical value that is characteristic of the material of the sample. This criterion indicates that the process responsible for the appearance of damage cracks is nonthermal in character.

2. The mechanical destruction caused by a laser in the free-running regime is similar to that caused by a Q-switched laser, which also indicates that the same process takes place in both cases.

3. The damage is not associated with electrical breakdown in the electromagnetic field of the laser radiation.

4. The light accompanying the appearance of damage is localized in microregions, is thermal in character, is delayed with respect to the beginning of damage development, and is not luminescence.

DISCUSSION

1. "The reason for threshold phenomena. The damage is determined by two types of processes: physical interaction of radiation with the substance and mechanical development of damage cracks. We shall show that the threshold values are determined by the mechanical process. We start from the firmly established fact that under the action of laser radiation cracks in amorphous polymers develop under the action of a gas that fills the internal cavity of the crack (5,6). (We leave aside for now the question of where the gas comes from). ···

2. Physical meaning of the damage criterion. The principal problem of laser damage of amorphous polymers is to explain the formation of gas. Unfortunately, it is not presently possible to solve this problem completely. ···The nonlinear dependence of the destruction on the intensity of the laser pulse shows unequivocally that the gas is not formed by a thermal process. The damage criterion can be interpreted in the following way. The mechanical requirement that specifies the threshold pulse assumes the formation of a definite quantity of gas Δm at the time of the laser pulse···, which is in practice determined by the number of polymer molecular bonds ruptured per second·····Since the

experiments showed that the damage is determined in the first place by the intensity of the laser radiation and not by the energy of the pulse, the assumption of multi-quantum processes of gas formation can be considered justified. Thus, from mechanical requirements that determine the development of cracks of critical size, a critical damage condition flows naturally; the rate of formation depends on multi-quantum processes of the interaction of laser radiation with a solid. Since the theory of the interaction of laser radiation with solids is not developed, we are limited to just these assertions...

3. Microregion emission. One of the most significant experimental facts presented above is the independence of the processes of crack formation and the emission from them: the emission begins after the crack has already begun to grow and develops independently. We believe that the microregion emission is dielectric breakdown. The phenomenon of dielectric breakdown by an electric field is well known, but little studied (11). ...In the polymers we used, there is a large number of micropores with dimensions less than 1 μm, ...one would suppose that under the action of laser radiation on the polymer samples breakdown will occur in them.....It is probably this type of breakdown that produces emission in microregions for subthreshold intensities. At the moment of formation of damage cracks in the sample, a cavity is formed filled with gas the pressure of which falls with time (as the crack grows). In this case breakdown is possible in this cavity. After 10 ns (delay time of the thermal emission) the crack has grown by 20 - 40 μm, and according to the estimates above, the gas pressure is not more than 100 atm. If the electrical discharge fills the entire cavity, the maximum size of the light-emitting region is 50 to 100 μm, which is the size observed experimentally (1); the minimum size is about 0.8 μm and will determine the cooling of the discharge-heated gas, which also agrees with experiment."

Agranat et al. attribute their damage threshold to the onset of multiphoton processes, but they do not know the nature of these. Nor do they have a perspective on why the light emission does not follow the laser pulse shape nor why the length of the pulse is unimportant. According to our model, the probable role of the multiphoton process is to cause a high excess electron density. Thus electrons are excited by the multiphoton process in sufficient number that a high local excess charge density is produced. This, in turn, starts bond-breaking and the chain reaction. Once the chain reaction is started, it is self-sustaining for a considerable time. Ultimately, the loss mechanisms dominate and the process stops. Two types of light emission have been distinguished by Agranat et al., a diffuse emission of low intensity that occurs on

subthreshold pulsing and which follows a 6500°K spectrum, localized to the regions of cavity formation that does not follow the waveform of the incident pulse. Neither could be associated with electroluminescence. Cooper and Elliott also distinguish two types of radiation: a diffuse and an intense. These will be described in some detail in the next section. The similarity of the light emission for laser and electrical breakdown is striking. From the point of view of the model, the diffuse emission is probably that of the highly excited atoms upon bond rupture. Apparently, this occurs over a relatively broad region without the chain reaction being initiated. Once the chain reaction is initiated, gas forms at high pressure and this gas emits its thermal spectrum. The time in which it is emitting is the time in which the atoms in the cavity are in the gaseous state. This is determined by the duration of the chain reaction and not the length of the original laser pulse.

(2) Light Emission. In the light emission study of Cooper and Elliott [5] on doubly recessed KBr single crystals, light was first observed about 20 nsec prior to voltage collapse. This was in the form of a "faint haze, variable in width, with a brighter central region or core. The photo-densitometer plots exhibit two regions, one starting at the cathode and penetrating into the material in which the exposure is approximately constant, and a second region in which the exposure falls towards the anode. The transition between the two regions occurs at different points for different specimens." The light at 15 nsec before voltage collapse was described as follows. The features previously seen were still present, but with increased intensity, and several new features appeared. "The bright core extends about half-way across the specimen, or beyond; there is now a bright region near the anode and one or more further cores have appeared in the haze." The authors offer two possible explanations of the bright region near the anode. The first is that "the core propagates from cathode to anode, the light emission from the tip increasing up to about half-way across the specimen, the intensity of the emission then falls and rises again as the anode is approached." The second explanation is that "a core grows out from the anode to meet that approaching from the cathode, the anode core beginning when the core from the cathode is about half-way across the specimen." The authors favor the first explanation.

At about 10 nsec before voltage collapse, the bright central core bridges the specimen completely and the haze surrounding it contains several other cores and is comparable in width with the specimen thickness. At 5 nsec before voltage collapse, the central core becomes very bright with no corresponding increase in intensity of the hazy region. In many cases, the core now shows several regions of brightness along its length giving the appearance of a beaded structure. There are several reasons for believing that the current through the specimen is large enough to produce permanent damage to the material of the core

at this stage. The closure of the shutter is within a few nanoseconds of the collapse of voltage. The diameter of the core is about 0.004 cm, which is the same as the diameter of the channels in the specimen after breakdown. Finally, the photographs in the early groups show several cores, yet Cooper and Smith found that the occurrence of a partial channel alongside the main channel was a rare event, which indicates that no permanent damage is produced by the cores in earlier stages, or by the haze at any stage.

Cooper and Elliott [36] explored directional effects of breakdown in strained and annealed KCl single crystals with double-recess type specimens oriented with their [110] direction parallel to the applied field. With the shutter closed at times between 15 and 10 nsec before the voltage collapse, light was emitted from a broad band across the specimen. The band was at an angle of approximately 45 degrees to the electrode surfaces in the case of the annealed specimens and perpendicular to the electrodes in the case of the others. In both cases the channel produced by the discharge lay in a narrow region of the specimen coincident with the center of the region from which light emission had occurred. In another specimen prepared so that the field direction was slightly off the [110] direction, the resolved field component along the [100] direction was significantly greater than the field component along the [010] direction. Light emanated from a small portion of the anode along both the [100] and the [010] directions. Only a diffuse haze was emitted along the [010] direction, while a bright core passed through the stronger haze in the [100] direction. This core had a zig-zag portion, the directions going from [100] to [010] and back to [100]. The discharge channel was produced along this core and there was no damage within the other (weaker) discharge. One conclusion drawn from the experiment was that the permanent damage to the specimens does occur in the path of the electronic instability, thus supporting the conclusion of Cooper and Fernandez that preferentially directed discharge channels correlate with an anisotropy in the electric strength. The existence of electronic instabilities in the directions other than the direction of the applied field also appears to rule out breakdown theories of the hot-electron type (the collective-electron theory of Frohlich and Paranjape, for example). The electric strengths of annealed specimens were between 0.60 and 0.80 MV/cm, while those for strained specimens were between 1.1 and 1.5 MV/cm.

Cooper and Pulfrey [7] found that the time at which light was first detected was about 20 nsec prior to voltage collapse independent of the waveform of the applied voltage when the rise rate was varied from 10^3 V/sec to 10^9 V/sec (rise time 30 sec down to 30 μsec). However, if the temperature were lowered to -50°C, no light emission was observed until about 3 nsec before voltage collapse. The light emission could not be attributed to a normal electroluminescence. They interpret the reduced time between light emission and breakdown as a speeding up of the breakdown process which could possibly be associated with an increase in electron mobility with decrease in temperature.

The results of Cooper and Agranat and their co-workers seem to be consistent with each other. Two types of light emission are identified, one that is hazy and is a precursor to the second. In each case, the precursor is shown to be different from the normal electroluminescence effect and no macroscopic damage can be found in the regions of hazy emission. Neither has determined the spectrum of this emission. The intense emission following the precursor is localized in each case to the regions of breakdown damage. Agranat et al. conclude that this emission is thermal, having a characteristic temperature of 6500°K.

The light emission observed by Budenstein and his co-workers [8] was in thin film systems rather than bulk. Precursors were not observed, but the observations were made perpendicular to the plane of the capacitor system, not looking directly into the dielectric as was done in the bulk experiments. The emission, then, represented the light that had either penetrated the thin film electrodes or emerged where these electrodes were vaporized or blown back by the breakdown. The electrodes were typically several thousand angstroms thick and can be regarded as completely opaque. Thus the emerging light implied electrode rupture. The emerging light signal begin within a few tens of nanoseconds (the limit of experimental resolution) of the time in which the voltage waveform indicated breakdown conduction was beginning. The waveform of the light intensity did not correlate in other details with the voltage waveform during breakdown conduction. Finally, a line spectrum was observed, not a thermal spectrum as reported by Agranat et al., for their strong emission accompanying laser damage.

The temperature estimated by Agranat et al. is presumably based on the observed spectrum of the breakdown light emission, although no details are presented to assure this is the case. In arriving at the temperature estimate for the gas in the discussion of the proposed breakdown model, we were strongly influenced by several factors: the lack of a thermal spectrum in the thin film studies, the strong evidence that conduction occurred by way of a gaseous channel, and the estimates on energy release per atom upon bond breakage and energy loss by heat conduction. If we assume that the experimental results as described are correct, there is an apparent conflict in the reporting of line spectra in the thin film studies and thermal spectra in the laser damage studies. The conflict can be reconciled with the proposed model. In the bulk system, the gas is confined as the channel grows. Frequently the period of conduction through the gas is so short that the pressure in the channels remains very high for that period. In thin films and in bulk systems, there is definite evidence for a very high pressure (see Section g), but the light emission shows that electrode rupture in thin film breakdown occurs very early in the breakdown process. Thus much of the conducting period occurs with the pressure greatly released and the spectrum is determined primarily by the atoms that are freshly released by bond rupture. For the confined gas, the emission is primarily by the bulk of high temperature gas atoms, the number of atoms within the volume being much greater than the number of the surface.

The connection between the hazy emission and the proposed model is not clear. In the proposed model, a critical charge density, bond rupture, chain reaction, and channel development are the essential steps. The haze might indicate that a high electron density is developing with some electrons in excited states that can decay by emission of radiation. The expected spectrum would then be characteristic of the energy level structure of the solid, i.e., broad peaks which sharpen as temperature is lowered and which should be sensitive to impurities and imperfections. However, the hazy emission might be associated with localized bond rupture, the emission coming from the freed atoms. Then line spectra should be observed (with considerable pressure broadening). The same is true if the chain reaction starts, but is quenched before the cavity size becomes so large that the number of volume atoms greatly exceeds the number of surface atoms. If gaseous regions were formed that were no more than a few hundred angstroms in diameter and these were rapidly quenched forming a glassy solid, optical measurements would almost certainly reveal no damage. Even if cavities of a few hundred angstroms diameter were formed, these would be very difficult to detect optically. Thus the hazy emission is not inconsistent with the proposed model.

The directional effects observed for the hazy emission by Cooper and Pulfrey require further study; it does not seem fruitful to speculate on their cause until more is learned about the emission itself.

(3) Role of Impurities, Imperfections, Voids, and Electrode Protrusions. Cooper et al. [41] have shown that substantial impurities in alkali halide single crystals produce little effect on the electric strength. The proposed model suggests that isolated impurities would not greatly influence the excess charge density over a region of several atoms. The impurity would probably cause local strain, but it may or may not cause a decrease in average bonding strength. Fracture resistance would probably be unaffected in single crystals having well-dispersed impurities.

Cooper and his co-workers [13] have also investigated breakdown thresholds in annealed and unannealed single crystals of KCl. With 55 unannealed specimens, the electric strength varied between 0.5 and 1.55 MV/cm, while the 43 annealed specimens varied from 0.5 to 1.25 MV/cm. The peak of the distribution for annealed specimens was at 1.2 MV/cm, while the peak of the annealed distribution was at 1.1 MV/cm, the shift being clearly visible in the data. In the proposed model, the higher breakdown strength of the unannealed specimens may be associated with the greater fracture resistance of these specimens. The annealing procedure may have decreased the dislocation density and increased the density of vacancies. When mechanical pressure was applied to annealed crystals, the entire distribution shifted toward higher breakdown fields: minimum 0.8 MV/cm, peak 1.3 MV/cm, and maximum 1.7

MV/cm. Since external pressure effectively increases bond strength and makes crack propagation more difficult, the pressure effect is understandable in terms of the proposed model.

Voids are macroscopic cavities in solids filled with gas. Ionization can occur within the gas before the breakdown threshold field is reached in the surrounding solid material. When ionization does occur, electrons impinge on the walls of the void and, according to the proposed model, can break the bonds of the wall atoms. If the electron density is relatively low, then a slow erosion process should occur. In a long period this could lead to the eventual failure of the system. As the cavity grows, the local field in the dielectric becomes greater for a given applied voltage to the system because the ionized void is a relatively good conductor. Eventually, the high field at the extremity of the cavity (which might be very tenuous and in the form of a tree) will cause sufficient electrons to be injected into the solid that the chain reaction is initiated. Then complete breakdown will occur.

Electrode protrusions, according to the proposed model, would be effective in initiating breakdown because of the high space charge produced in their vicinity when the electric field is sufficiently high. This space charge would, in turn, initiate the bond disruption and chain reaction.

(4) Other Aspects

(a) Evidence of High Gas Pressure. In the proposed model, gas at an extremely high pressure is assumed to exist in the interior of the insulator as the chain reaction progresses. Evidence has been cited to substantiate the existence of a high pressure during breakdown [33]. Additional direct evidence comes from thin film experiments. Hayes [8] deposited a layer of copper several micrometers thick onto a glass substrate. On top of this was a layer of SiO about 0.2 μm thick and an upper electrode of Al of about 0.1 μm. Measurements revealed the configuration shown in Figure 10. The observed deformation of the copper, which occurred during the several microseconds of breakdown conduction, indicates that extremely high pressures were involved. The "blown back" appearance of the outer electrode and the acoustical disturbance produced by breakdown are further evidences of the high gas pressure accompanying breakdown in thin film systems.

(b) Temperature Dependence at Breakdown Strength. Most studies show that the dielectric strength decreases slightly with rising temperature (here we are not concerned with the high temperature region where insulators change into semiconductors). Avalanche theories generally predict that the breakdown field should rise with increasing temperature because of the difficulty in getting an avalanche initiated in the presence of many electron-phonon collisions. In the proposed

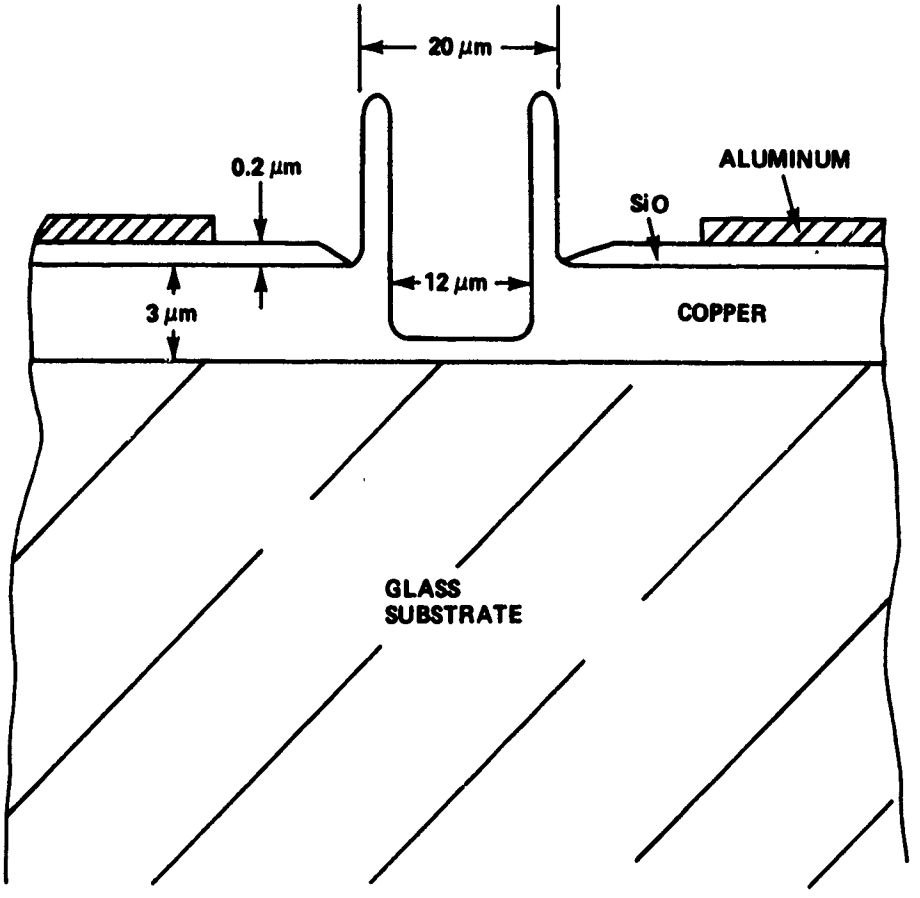

Figure 10. Section through a breakdown in a thin film Cu-SiO-Al thin film capacitor showing the deformation in the copper layer due to the high pressure accompanying dielectric breakdown [8].

model, a decrease in breakdown voltage with increasing temperature is plausible because bonding strengths decrease with increasing temperature. Cooper [13] has shown that there is a rough correspondence between the shapes of the breakdown field versus temperature and Young's modulus versus temperature curves for many materials. The situation is not clear cut, however, since the fracture properties of materials vary in a complicated fashion with temperature and with the type and density of imperfections.

(c) Thickness Dependence of Breakdown Strength. In the proposed model, the initiation of breakdown would depend largely on the rate at which space charge of the critical density forms. Thus, theories of prebreakdown conduction describing the formation of space charge may well include thickness dependence of the breakdown strength.

(d) Effect of Dielectric Constant on Breakdown Strength. Materials with high dielectric constants seem to have systematically lower breakdown strengths than materials with low dielectric constants. High dielectric constants in solids are associated intimately with the crystal structure. If this structure is randomized, then the dielectric constants fall. Previously, we have suggested that the hazy emission of Cooper, Agranat, and their co-workers might indicate that the chain reaction was occurring, but that the system was quenched before the gaseous region became very large. For a material of high dielectric constant, the gas would be of low dielectric constant. Hence, the cavity wall would contain a high polarization charge density and the cavity an enhanced field. Both of these effects would tend to speed up the reaction rate and hence lower the field for breakdown.

(e) Polarity Effect. For point-plane geometries, KBr specimens broke down at 0.36 MV/cm for positive point and 0.47 MV/cm for negative point (fields computed by dividing the breakdown voltage by the electrode separation) [6]. Davisson [3] indicates that the breakdown patterns with positive point are indistinguishable from those with negative point. Since the lower breakdown voltage occurred for positive point, the proposed model indicates that a greater space charge develops about a positive point than a negative point. The mechanisms for development of the space charges could involve electrode emission (electrons or holes), avalanche multiplication, or other processes. Cooper and Pulfrey [7] show that processes involving ion transport are very unlikely.

In thin film capacitors, the breakdown strength generally is polarity sensitive, but it is not easy to predict which polarity will give the lower average breakdown voltage. The cause of the polarity sensitivity is probably the nonuniformity of the thin films, relatively small variations in the conditions of deposition making one dielectric-metal interface rougher than the other. This roughness, in turn, will influence the rate at which space charge is formed within the dielectric and hence the point of initiation of the chain reaction of the proposed model.

(f) Voltage Breakdown Waveform. Pulfrey and Bradwell [6] measured the time for voltage collapse for KBr specimens of the type employed by Cooper and for polythene specimens. The time for voltage collapse (100 to 0 percent) was 4.5 ± 0.5 nsec for KBr specimens and 0.8 ± 0.1 nsec for polythene specimens, with breakdown strengths of 0.57 MV/cm and 6 MV/cm, respectively, for uniform field geometries. The specimen thicknesses were 0.05 cm for KBr and 0.005 cm for polythene. The authors indicate that the collapse of voltage occurs in the time taken for the ionized channel between the electrodes to develop into a highly conducting plasma. The onset of the relief wave occurring at breakdown is very abrupt for polythene (less than 0.1 nsec). The KBr waveform exhibited three slopes: a slowly falling voltage for

about 4 nsec, a rapidly falling voltage for 1 to 2 nsec, and, finally, a gradually falling voltage for about 5 nsec. The first region might be associated with conduction through the original channel through the system, the second by channel enlargement due to Joule heating, and the third to further increase in conductance as the pressure is released and the mean free path of electrons increases.

The rapid change of resistance on dielectric breakdown is the basis for the solid dielectric switch; a switching time of about 0.1 nsec can be achieved for fast-rising voltages and point-plane electrodes separated by 1 mm of polyethylene. If crack propagation is an important aspect of the channel growth, then the crack propagation velocity necessary for 0.1 nsec switching must be several thousand times the speed of sound in the dielectric. Studies of crack propagation in metals indicate that the crack velocity is generally no more than 0.3 times the speed of sound in the medium. Thus the formation of a gaseous channel from point to plane may seem contradictory to the proposed mechanism. One way of rationalizing the observations is to hypothesize that the electron injection from the electrode point is so intense and penetrating that the critical charge density is reached almost simultaneously throughout the thickness of the dielectric and the chain reactions starts almost simultaneously so that crack propagation plays little or no role in the formation of the channels.

In thin film systems, the same specimen can be made to undergo many breakdowns because each breakdown leaves the system unshorted and the damaged area effectively isolated. The voltages employed are quite small (say, 30 to 100 V) compared to the voltages employed in the study of bulk dielectrics (say, 1 to 200 kV). Also, the capacitance of the test system is much smaller for the bulk case than the thin film case and the circuital conditions quite different. It is easy to arrange circuit parameters in the thin film case so that the capacitor is effectively isolated from its voltage source during the time that breakdown is occurring. Examination of the waveform of the thin film capacitor accompanying breakdown shows that the voltage falls to a well-defined value for a particular capacitor and, whereas the voltage for the onset of breakdown fluctuates considerably, the voltage at which breakdown conduction ceases is much more narrowly defined [8]. The voltage is typically between 10 and 20 V, regardless of capacitor thickness (in the range 1000 to 10,000 Å) or voltage polarity. The voltage of the cessation of breakdown is typically polarity sensitive for a given capacitor, varying by several volts. A high voltage for the onset of breakdown goes with a high voltage for the cessation of breakdown conduction. In the model proposed, conduction occurs through the gas that bridges the electrodes. When it is no longer possible to keep the gas ionized, conduction should cease. We associate the terminating voltage with an ionization threshold. The polarity effects indicate that a more elaborate explanation is required to give a complete account.

4. Summary

A model for dielectric breakdown in solids has been proposed wherein the breakdown process is divided into five stages: creation of a critical charge density, bond disruption, chain reaction, growth of a gaseous cavity and crack formation, and completion of the gaseous channel bridging the electrodes and conduction through this channel. A simplified model was formulated to illustrate the kinetics of the process and the model was examined from several points of view. The model seems to provide a good perspective on the common features of breakdown induced by electric, electron beam, and laser beam excitations. Considerations of the rate of heat transfer led to estimates (upper limits) of the time scale of breakdown. The model provides meaningful perspectives on the light emission accompanying breakdown, on the geometric configuration of breakdown patterns, on the roles of inhomogeneities, voids and electrode projections, and other significant aspects of breakdown.

The proposed model must be regarded as speculative. Required is a detailed analysis of the phenomenological model and a quantum mechanical treatment to show how space charge produces (or fails to produce) bond disruption. Additional experimentation is needed to clarify the light emission phenomena, to determine clearly when the gaseous channel is completed, and to relate channel growth to conduction through the system. Both the theoretical and the experimental questions are being further pursued.

REFERENCES

1. Whitehead, S., Dielectric Breakdown of Solids, Clarendon Press, Oxford, 1951.

2. Mason, J. H., "Dielectric Breakdown of Solid Insulation," Progress in Dielectrics, 1, J. B. Birks and J. H. Schulman (Editors), John Wiley and Sons, Inc., New York, 1959, pp. 1-58.

3. Davisson, J. W., "Directional Breakdown Effects in Crystals," Progress in Dielectrics, 1, J. B. Birks and J. H. Schulman (Editors), John Wiley and Sons, Inc., New York, 1959, pp. 59-96.

4. Kreuger, F. H. Discharge Detection in High Voltage Equipment, American Elsevier Publishing Company, Inc., New York, 1965, pp. 1-8.

5. Cooper, R., and Elliott, C. T., "Formative Processes in the Electric Breakdown of Potassium Bromide," Brit. J. Appl. Phys., 17, 481-488, 1966.

6. Bradwell, A., and Pulfrey, D. L., "Time of Breakdown in Solid Dielectrics," Brit. J. Appl. Phys. (J. Phys. D.), 1, 1581-1583, 1968.

7. Cooper, R., and Pulfrey, D. L, "Discharge Propagation through Single Crystals of KBr," J. Phys. D., 4, 292-297, 1971.

8. Budenstein, P. P., Hayes, P. J., Smith, J. L., and Smith, W. B., "Destructive Breakdown in Thin Films of SiO, MgF_2, CaF_2, CeF_3, CeO_2, and Teflon," J. Vac. Sci. and Technol., 6, 289-303, 1969.

9. Agranat, M. B., Krasyuk, I. K., Novikov, N. P., Perminov, V. P., Yudin, Yu. I., and Yampol'skii, P. A., "Destruction of Transparent Dielectrics by Laser Radiation," Soviet Physics JETP, 33, 944-948, 1971.

10. Yablonovitch, E., "Optical Dielectric Strength of Alkali-Halide Crystals Obtained by Laser-Induced Breakdown," Appl. Phys. Lett., 19, 495-497, 1971.

11. O'Dwyer, J. J., "The Theory of Avalanche Breakdown in Solid Dielectrics," J. Phys. Chem. Solids, 28, 1137-1144, 1967.

12. Vorob'ev, G. A., Mukhachev, V. A., and Rudnev, A. N., "Breakdown Mechanism in a Silicon Monoxide Film," Soviet Physics-Technical Physics, 13, 1575-1580, 1969.

13. Cooper, R., "The Electric Strength of Solid Dielectrics," Brit. J. Appl. Phys., 17, 149-166, 1966.

14. Smith, J. L., and Budenstein, P. P., "Dielectric Breakdown in Thin Evaporated Films of CaF_2, MgF_2, NaF and LiF," J. Appl. Phys., 40, 3491-3498, 1969.

15. Klein, N., "A Theory of Localized Electronic Breakdown in Insulating Films," Adv. in Phys., 21, 605-645, 1972.

16. Simmons, J. G., DC Conduction in Thin Films, Mills and Boon Ltd., London, 1971.

17. Simmons, J. G., "Conduction in Thin Dielectric Films," J. Phys., D4, 613-657, 1971.

18. O'Dwyer, J. J., The Theory of Electrical Conduction and Breakdown in Solid Dielectrics, Oxford University Press, London, 1973.

19. Watson, D. B., "The Impulse Electric Strength of Polythene as a Function of Voltage Risetime," J. Phys., D4, L19-L20, 1971.

20. Bradwell, A., Cooper, R., and Varlow, B., "Conduction in Polythene with Strong Electric Fields and the Effect of Prestressing on the Electric Strength," Proc. Inst. Elec. Eng., 118, 247-254, 1971.

21. Mukhachev, V. A., and Mukhacheva, N. S., "The Temperature Dependence of the Electrical Strength of Silicon Monoxide Films," Izv. VUZ Fiz., No. 11, 155-157, 1970.

22. O'Dwyer, J. J., The Theory of Dielectric Breakdown of Solids, Oxford University Press, London, 1964.

23. Vorob'ev, G. A., "Mechanism of Dielectric Breakdown in Films," Soviet Physics--Solid State, 10, 203-204, 1968.

24. Vershinin, Yu. N., "Instability of a Plasma During Electrical Breakdown of Solid Dielectrics," Soviet Physics--Solid State, 11, 688-689, 1969.

25. Bowden, F. P., and McLaren, A. C., "The Explosion of Silver Azide in an Electric Field," Proc. Roy. Soc., A246, 197-199, 1958.

26. Chaudhri, M. M., "High Speed Photography of Electrical Breakdown and Explosion of Silver Azide Crystals," Nature Physical Sci., 242, 110-111, 1973.

27. Fischer-Hjalmers, Inga, "Ground State and Low Excited States of the Negative Hydrogen Molecule Ion," Arkiv for Fysik, 16, No. 4, 33-55, 1958.

28. Eliezer, I., Taylor, H. X., and Williams, J. K., Jr., "Resonant States of H_2^-," J. Chem. Phys., 47, 2165-2177, 1967.

29. Benson, S. W., The Foundations of Chemical Kinetics, McGraw-Hill Book Company, Inc., New York, 1960, p. 54.

30. Budenstein, P. P., and Hayes, P. J., "Breakdown Conduction in Al-SiO-Al Capacitors," J. Appl. Phys., 38, 2837-2851, 1967.

31. Field, F. H., and Franklin, J. L., Electron Impact Phenomena, Academic Press, Inc., New York, 1957.

32. Carslaw, H. S., and Jaeger, J. C., Conduction of Heat in Solids, Oxford University Press, London, 1959, pp. 341-343.

33. Zlatin, N. A., Kozhushko, A. A., Lagunov, V. A., and Stepanov, V. A., "Pressure in the Discharge Channel Produced by Breakdown of a Solid Dielectric," Soviet Physics--Technical Physics, 17, 2037-2038, 1973.

34. Steverding, B., "Thermomechanical Damage by Pulsed Lasers," J. Phys., D4, 787-792, 1971.

35. Yokobori, T., An Interdisciplinary Approach to Fracture and Strength of Solids, Wolters-Noordhoff Scientific Publications Ltd., Groningen, The Netherlands, 1968, pp. 153-154.

36. Cooper, R., and Elliott, C. T., "Directional Electric Breakdown of KCl Single Crystals," J. Phys., D1, 121-123, 1968.

37. Trump, J. G., and Wright, K. A., "Injection of Megavolt Electrons into Solid Dielectrics," Mat. Res. Bull., 6, 1075-1083, 1971.

38. Milton, O., Private Communication.

39. Lowrie, R., Private Communication.

40. Starodubtsev, S. V., and Romanov, A. M., The Passage of Charged Particles Through Matter, Israel Program for Scientific Translations, Jerusalem, Israel, 1965.

41. Cooper, R., Higgin, R. M., and Smith, W. A., "The Influence of Ionic Conductivity on the Electric Strength of KCl and NaCl," Proc. Phys. Soc., London, B76, 817-825, 1960.